

REVIEW

# Structural Image Analysis of the Brain in Neuropsychology Using Magnetic Resonance Imaging (MRI) Techniques

Erin D. Bigler<sup>1,2,3</sup>

Received: 30 April 2015 / Accepted: 16 July 2015 / Published online: 18 August 2015  
© Springer Science+Business Media New York 2015

**Abstract** Magnetic resonance imaging (MRI) of the brain provides exceptional image quality for visualization and neuroanatomical classification of brain structure. A variety of image analysis techniques provide both qualitative as well as quantitative methods to relate brain structure with neuropsychological outcome and are reviewed herein. Of particular importance are more automated methods that permit analysis of a broad spectrum of anatomical measures including volume, thickness and shape. The challenge for neuropsychology is which metric to use, for which disorder and the timing of when image analysis methods are applied to assess brain structure and pathology. A basic overview is provided as to the anatomical and pathoanatomical relations of different MRI sequences in assessing normal and abnormal findings. Some interpretive guidelines are offered including factors related to similarity and symmetry of typical brain development along with size-normalcy features of brain anatomy related to function. The review concludes with a detailed example of various quantitative techniques applied to analyzing brain structure for neuropsychological outcome studies in traumatic brain injury.

**Keywords** Magnetic resonance imaging · Image analysis · Voxel-based · FreeSurfer · Size-function

“Every Behavior has an Anatomy” Norman Geschwind, M.D. (1975)

Geschwind’s statement highlights why understanding neuroanatomy is so important for neuropsychology. Indeed, anatomy has always been a starting point for medicine as well as neuropsychology. The foundation of neuropsychology begins with structural neuroanatomy and its relation to cognition and behavior (Hécaen and Albert 1978). Unlike the past where neuroanatomy was strictly a topic of post-mortem studies, gross neuroanatomy can now be studied and taught via neuroimaging (Drapkin et al. 2015). Current advancements in the field of neuropsychology are intimately tied to neuroimaging and techniques that assess the structural integrity of the brain. This review will highlight contemporary methods used in imaging gross brain anatomy, with an emphasis on techniques that have become more automated. It will begin with a historical perceptive.

Neuropsychology began in an era where brain pathology could only be inferred in the living individual short of neurosurgery or some sort of open head wound as exemplified by the historical case of Phineas Gage and the tamping iron that was blown through his left frontal lobe (Haas 2001). Other cases of open head injuries and alteration in behavior began to be reported after the first and second World Wars (see review by Shah et al. 2015). These head injury survivors created the natural laboratory to study the effects of brain injury and how to reliably assess changes in cognition and behavior (Tooth 1947; Zangwill 1945). Open head wounds and what could be surmised from focal traumatic injuries to the head during wartime provided the backdrop for some of the first

✉ Erin D. Bigler  
erin\_bigler@byu.edu

<sup>1</sup> Department of Psychology, Brigham Young University, Provo, UT, USA

<sup>2</sup> Neuroscience Center, Brigham Young University, Provo, UT, USA

<sup>3</sup> Department of Psychiatry, University of Utah, Salt Lake City, UT, USA

lesion-localization studies that became the early foundation for neuropsychological inference (see historical reviews by Collins 2006; Eling 2015). The work of Alexander Luria exemplifies this era of neuropsychological inference about neuroanatomical and neuropathological correlates (see Glotzman 2007). Cases with documented focal lesions, some directly observed in the battlefield, formed part of the basis for Luria's influential 1962 magnum opus on "Higher Cortical Functions in Man (Luria 1962)." Luria's text is a remarkable contribution to the field of neuropsychology with important insights to brain function that continue to generate testable hypotheses today (Christensen et al. 2009). However, all of Luria's work predated contemporary neuroimaging so the only simultaneous observation of a patient's brain and related neuropsychological function came by way of inference. Shallice (1988) referred to this era of neuropsychology as a time of 'diagram making' since conceptualization of brain-behavior relations could be diagrammed but without neuroimaging, never shown in the context of the patient's own neuroanatomy and neuropathology while alive. The 'Higher Cortical Functions' book has only diagrams. Nonetheless, Luria was keenly aware of systematically relating behavior back to some presumed region of neural control that was anatomically based.

Prior to about the mid-1970s without an image of the brain how could researchers directly study the effects of damage, especially concerning the extent of neuropathology and its relation to neuropsychological outcome in the living individual? For neuropsychology in the 1950's and 60's, this took innovative methods using what by today's standards were very crude techniques. The research of Brenda Milner or Hans Lukas Teuber (see Akert and Warren 1964) exemplified these challenges. Both knew that psychometric examination of frontal lobe damage on cognition and behavior required some method to objectively map the pathoanatomical damage to the brain. This era was long before any non-invasive brain imaging technique.<sup>1</sup> Nonetheless, both used innovative approaches to establish frontal lobe damage in the living research subject. To substantiate presence of frontal damage, Teuber used military veterans injured in World War II or the Korean War who had sustained through-and-through frontal gunshot wounds (GSWs) as documented by skull x-ray films, the primary radiological method of the day. While the standard lateral skull films were used to infer where the presumed underlying frontal damage must be, no specific details of the frontal lesion could be examined. Milner used a different approach by quantifying the amount of frontal tissue removed from tumor patients undergoing resection for frontal lobe

neoplasm. Post-surgically either the resected tissue could be measured or the neurosurgeon would plot out the general region where brain parenchyma was removed. For neuropsychology to make some claim that a particular anatomical brain region related to some aspect of cognition or behavior it had to start with an anatomical description of what was damaged. The classic cases of anatomical description in early to mid-20<sup>th</sup> century neuropsychology had all relied on descriptions from post-mortem, post-neurosurgical or select cases of open head wounds, as described above.

The importance of knowing the anatomical pathology and structures affected in determining neuropsychological correlates, at least for 20<sup>th</sup> century neuropsychology was based on three key assumptions as summarized by Cipolotti and Warrington (1995): (a) a high degree of functional specialization occurs at the level of the cerebral cortex, (b) a modularity approach to the analysis of complex cognitive skills taps cortical areas associated with functional specialization and (c) systematic study of cases with selective damage within given cortical areas provides insights to neuropsychological correlates of cortical function. To accomplish this last point there needed to be an effective way to show where damage had occurred or some type of pathological change or deviation from normal anatomy. As will be discussed later in this review, these three assumptions came prior to the more elaborate contemporary network theories of cognitive functioning which fortunately 21<sup>st</sup> Century neuroimaging has the potential to address.

## Overview of Structural Neuroimaging Analyses

Hounsfield's (1973) first publication on computed tomography (CT) was 1973. It took another 4 to 5 years before the first published neuropsychological studies used CT imaging to clinically define pathology such as degree or presence of atrophy or gross lesion localization (Botez et al. 1977; Dolinskas et al. 1978; Gonzalez et al. 1978; Naeser and Hayward 1978). These early studies merely reported a rater's impression about a visualized clinical finding, so no real quantitative analyses were performed. By the early 1980's linear measurements, basic volumetric measures and surface area computation began to be examined (Zatz et al. 1982a) and related to neuropsychological function including language (Naeser et al. 1981) and clinical samples of aging individuals (Zatz et al. 1982b) and those with dementia (Bigler et al. 1985), schizophrenia (Jernigan et al. 1982b), traumatic brain injury (TBI, Cullum and Bigler 1986) and alcoholism (Jernigan et al. 1982a, b, c).

Still with a lesion-localization focus the first textbooks on neuroimaging specifically related to neuropsychology were published in the 1980's and early 1990's (see Bigler et al. 1989; Kertesz 1984, 1994). While the beginnings of CT

<sup>1</sup> Pneumoencephalography (PEG) existed then but with high levels of mortality and morbidity it was not routinely used for head trauma. It only provided a silhouette of the ventricular system. Cerebral arteriography also existed but only provided a two-dimensional view of the cerebral vasculature and not the brain

imaging began to solve the problem of being able to coarsely identify lateralized lesions or abnormalities, subcortical structures were difficult to differentiate and CT was not sensitive to most subtle pathologies. In the 1980's nuclear medicine adapted CT technology to generate functional images of the brain based on radiopharmaceutical uptake using single photon emission computed tomography (SPECT) and positron emission tomography (PET). Despite these advances with CT imaging technology and even with the introduction of magnetic resonance imaging (MRI) in the 1980's, it was not until the 1990's that magnetic resonance (MR) technology improved to the point to where neuroimaging truly approached gross anatomy, as shown in Fig. 1. Figure 1 is actually an MR image of the author's brain compared to a postmortem section at approximately the same coronal level of a male cadaver donor, who died from non-neurological causes. The gross anatomical detail provided by contemporary MRI is remarkably similar to the visible postmortem brain.

Despite steady improvements in neuroimaging technology from Hounsfield's discovery in the late 1960's to early 1970's, it was not until about the last decade of the 20<sup>th</sup> Century that neuroimaging started to become an integral part of neuropsychological studies. Using the National Library of Medicine and applying the search words of "neuroimaging" and "neuropsychology" as shown in Fig. 2, MRI studies only slowly became a part of neuropsychological investigations. A major reason for this was that in the beginning of neuroimaging applications to neuropsychology any type of quantitative image analysis had to be done by hand, using laborious and time-intensive hand tracing techniques (Bigler 1996a, b). As methods for automation came online, this changed and as can be seen in Fig. 2, the last decade and a half shows

accelerated number of neuroimaging-neuropsychology investigations. In fact, any current study purporting to examine the role of some region of interest (ROI) relating brain structure to function, in 21<sup>st</sup> Century research would be incomplete without some neuroimaging measure of neuroanatomy, neuropathology, or both.

MRI is now well established and definitively the contemporary standard for structural image analysis, which is the focus of this review. As remarkable as Fig. 1 shows gross neuroanatomical detail from a living individual, it was immediately recognized that quantification of the structural brain image was needed for neuropsychology to effectively use this information in advancing brain-behavior associations. There are many treatises on image acquisition and clinical reading of neuroimaging findings, and they will not be the emphasis of this review. The focus of this review is on how quantitative neuroimaging analysis methods are used to develop relevant metrics for neuropsychology. First an overview on the development of quantitative imaging techniques, followed by some interpretive guidelines for image analysis and the review will conclude with an example of how multiple image quantification techniques can be obtained in a given subject and applied to neuropsychological outcome.

As already briefly overviewed, even though basic quantitative neuroimaging methods began to be used in the 1980's, most of the neuropsychological research that used neuroimaging during this era followed the pattern where brain imaging findings were merely used to compare and contrast patients with identifiable pathology of some type, verified either by CT or MRI. These studies required no sophisticated image analysis methods other than a trained rater specifying the type and location of pathology. In an attempt to better objectify areas and extent of damage (see Kertesz 1984, 1994), lesion overlap methods, as shown in Fig. 3, provided some quasi-quantitative indications of damage. Initially, this approach did not attempt to quantify, but rather showed broad regions of lesion involvement. With the advent of computer graphical analyses, however, computation of surface area, ventricular or lesion volume could be calculated, which marked the beginnings of computational methods for quantitative neuroimaging in neuropsychology (George et al. 1983; Pfefferbaum et al. 1988; Raz et al. 1987; Shimamura et al. 1988; Turkheimer et al. 1984; Walser and Ackerman 1977). Now both lesion mapping and quantification methods may be integrated using techniques like voxel-based lesion-symptom mapping (VLSM, Bates et al. 2003; see Fig. 3). The VLSM technique has been particularly helpful in exploring relations between focal lesions, typically from a cerebrovascular accident to neuropsychological function (Campana et al. 2015; Glascher et al. 2009, 2012; Robinson et al. 2014; Rogalsky et al. 2015).

Quantitative methods in the form of linear radiographic measures did pre-date CT imaging and were part of the analysis of air or pneumoencephalography (PEG) findings (Synek

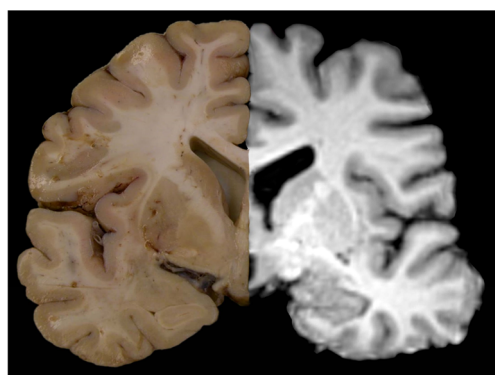


**Fig. 1** Post-mortem coronal section (viewer's left) compared to the author's T1-weighted MRI (viewer's right). Note the gross similarities indicating that the MR image approximates an actual brain. The post-mortem section was from a male in his 50's who donated his brain at the time of death which occurred from systemic disease with no known brain involvement. The MRI studies of the author's brain were obtained when he was 65. Some image distortion always occurs in post-mortem specimens since CSF is no longer pressurized (see Pfefferbaum et al. 2004). Post-mortem illustration was provided by Marc Norman, Ph.D



**Fig. 2** Using the article search engine provided by the National Library of Medicine ([pubmed.gov](#)) with the key search words of “neuroimaging” and “neuropsychology” as may be visualized, minimal levels of research

et al. 1976). PEG studies required that cerebrospinal fluid be drained from the ventricles and other brain cisterns and be replaced by air, allowing standard skull film x-ray to reveal a silhouette of the ventricle (Fig. 4). The width of the anterior horn of the lateral ventricle in relation to skull width (referred to as the Evans’ Index or Ratio) provided an index of ventricular size adjusted for head size, which was immediately

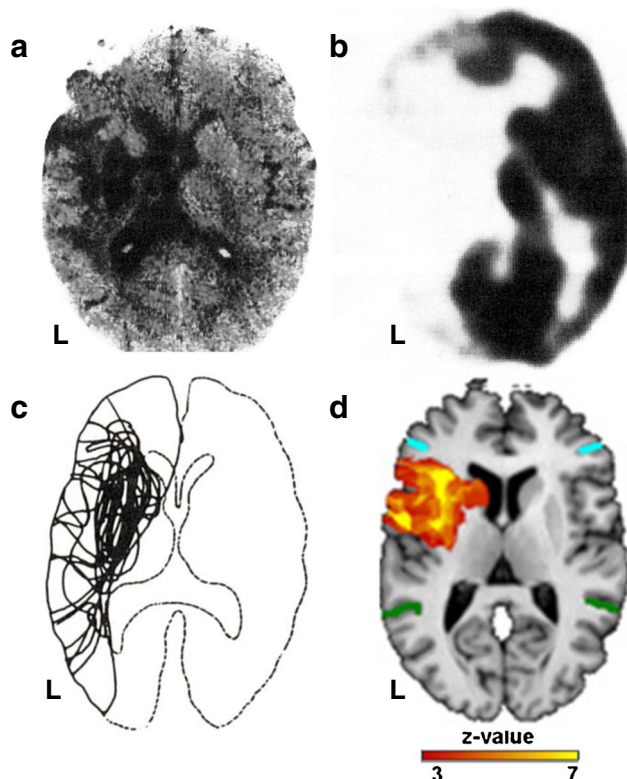


**Fig. 3** The images in A-C are from Kertesz (1994) used with permission. **a** Axial CT image circa early 1980’s depicting large peri-Sylvian atrophy secondary to infarction. **b** Positron emission tomography (PET) depicting large area of diminished to absent radiotracer uptake involving most of the left hemisphere. **c** Hand drawn lesion mapping where individual cases like that shown in A or B, is in turn drawn on a template. As can be seen the core overlapping region of these lesions/abnormalities is within the deep central core of the left hemisphere. **d** Computer based voxel-based lesion-symptom mapping (VLSM) of where lesion overlaps coincide with impaired verbal comprehension, taken from Glascher et al. (2009) used with permission. Although VLSM represents a more sophisticated and empirical method, note that even the older methods provided important localization information

on this topic occurred prior to the 21<sup>st</sup> Century. As of this writing approximately 1500 studies exploring neuroimaging and neuropsychology relations have been published

adapted for use in CT brain imaging, a measure that continues to be used today (Ragan et al. 2015). In cases of brain atrophy, the ratio would increase because ventricular expansion fills the void of parenchymal loss (referred to as hydrocephalus ex vacuo). Linear measures of landmarks, like the interuncal distance, sulcal or interhemispheric width or other measures using linear assessment of brain structure were applied to CT imaging (Grafman et al. 1986) or basic volumetric measures of sulci or the ventricles were obtained (Pfefferbaum et al. 1990). Certain pathologies would displace aspects of the lateral ventricle (like a space occupying lesion or edema), creating a midline shift. Thus, pathologies could be assessed with linear or surface area metrics in PEG or CT. Although these were the first kinds of metrics applied to studying brain structural abnormalities related to neuropsychological outcome (Booker et al. 1969; Matthews and Booker 1972), the coarseness of these kinds of measures is obvious. Nonetheless, an enduring marker of global atrophy is a derivative of the Evans’ index or ratio – the ventricle-to-brain ratio (VBR) where total ventricular volume is divided by brain volume and multiplied by 100 so that whole numbers are used in the quantification metric. The VBR is not only an established measure of overall brain integrity, but as a ratio it automatically adjusts (partially) for head size variation (Mathalon et al. 1993) and commonly relates to neuropsychological status (Bigler et al. 2013; Green et al. 2014; Olesen et al. 2011; Tate et al. 2011). Like all quantitative image techniques it is not without its drawbacks and there are circumstances where it may be best to adjust or correct for head size statistically (e.g., regression or covariance) rather than using a ratio like the VBR (Arndt et al. (Arndt et al. 1991)). Furthermore, in some disorders of brain development head size may become a dependent variable under investigation where no correction should be imposed. Since underlying component structures are positively related to overall brain volume, but not necessarily proportional in development there are complex brain size/intracranial size corrections that need to be considered in some analyses (Liu et al. 2014; Voevodskaya et al. 2014).

Fortunately, as MRI technology improved in terms of acquisition time, thinner slice thickness, and pixel resolution so did methods for image analysis. Anatomical MR images that

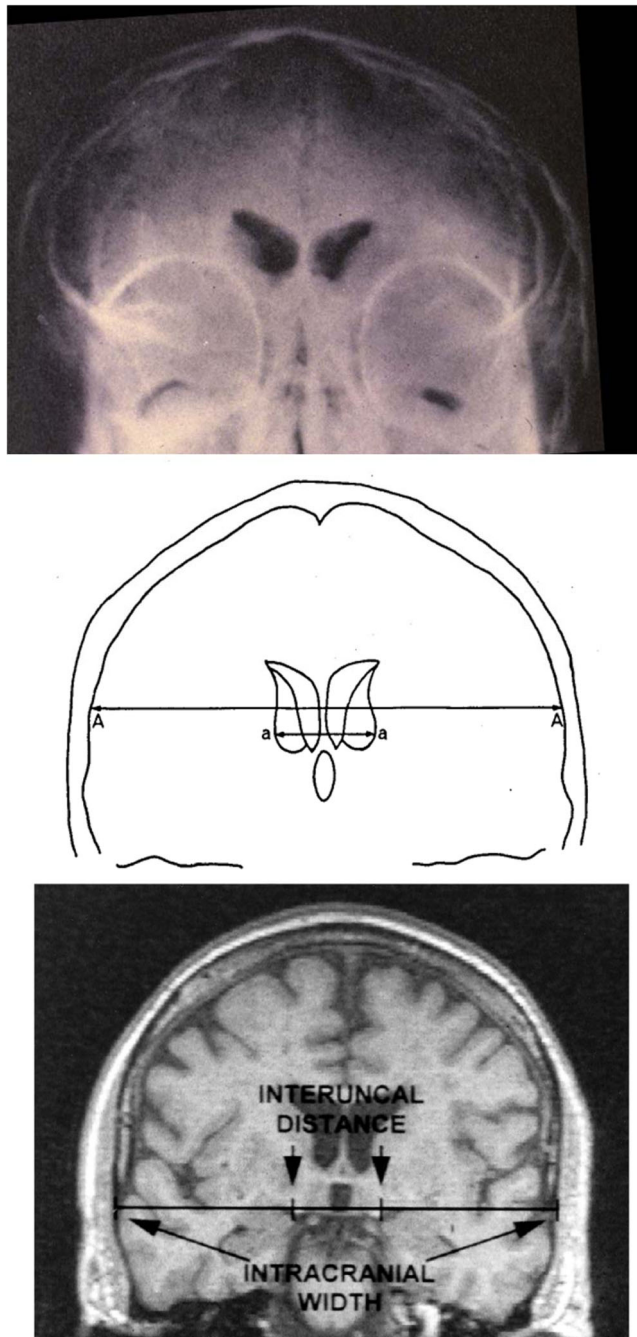
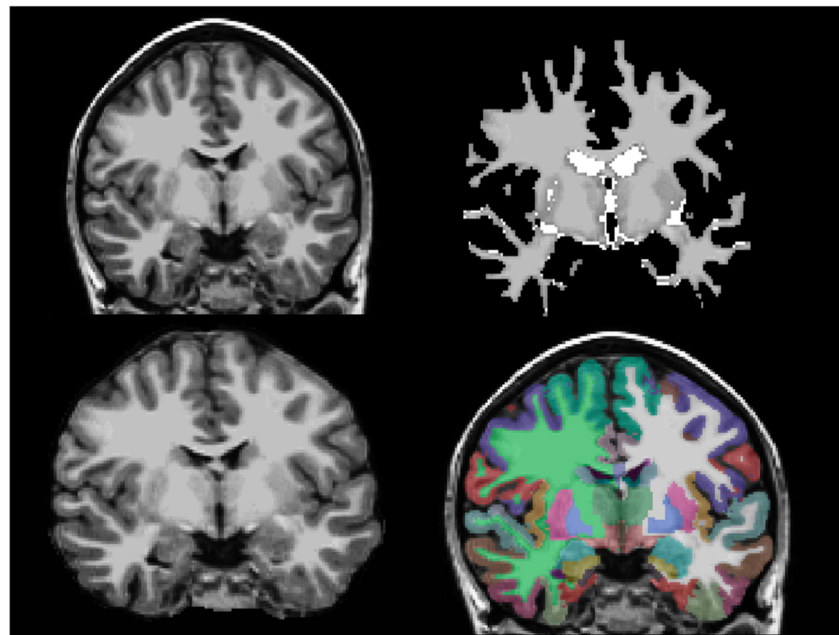


**Fig. 4** (Top) Air or pneumoencephalography (PEG) as taken from a frontal skull x-ray view. Note that with CSF removed and replaced with air, the lateral ventricle including the temporal horns are identifiable in the image. (Middle image) Outline drawing showing the lateral ventricle from PEG where the linear distance between the outer width of the lateral extent of the lateral ventricle (**b**) compared to the linear distance across the brain from the inner table of the skull (**a**) was used to derive a ratio of ventricular size to head size (from Synek et al. 1976; used with permission). Comparing these linear measures resulted in the Evans' index or ratio. (Bottom) Even with MRI, linear measures may still be useful as shown here where the width or distance between uncus to uncus compared to the invariant measure of the intracranial width, to generate an index of temporal lobe atrophy (from Laakso et al. 1995; used with permission). Also, note the Evans' Index can be derived with MRI just as it was with PEG

approached one millimeter thickness with minimal or no gap between slices meant more accurate volumetric quantification. For example, in the early 1990's, Shenton et al. (1992) and Zipursky et al. (1994) published some of the first studies using MRI that quantified various temporal lobe structures including the hippocampus but required operator-controlled tracing of the target region of interest (ROI). Other studies around the same time quantified multiple brain structures and ROIs but everything required laborious hand tracing (see Heindel et al. 1994; Shear et al. 1994) Furthermore, for scientific rigor all manual tracings required at least two independent raters, expertly trained to do the tracings so that inter-rater reliabilities could be established. Naturally, this was tedious, laborious, and time-consuming. For example, in a study published in 1997 by the author (see Bigler et al. 1997) on age-related changes in the hippocampus in comparison to those with TBI it took more than 50 h per subject to manually trace temporal lobe structures and whole brain morphology. Although these analyses were aided by computerized thresholding techniques that enhanced the gray scale image contrasts, the boundaries of all identifiable brain structures examined still had to be meticulously traced by hand. For these reasons, most pre-21<sup>st</sup> Century quantitative image analysis studies that examined a neuropsychological variable used simplified methods focused on one or a few ROIs. Fortunately, post-image acquisition techniques, referred to as post-processing techniques became more and more automated for tissue segmentation ultimately resulting in white matter (WM), gray matter (GM) and cerebrospinal fluid (CSF) classification of all major brain ROIs (Fig. 5). Although much of the post-processing is automated, the imaging files still need to be properly formatted for image analysis and once processed, checked for quality assurance. Additionally, during post processing there may be operator-controlled editing and other modifications (i.e., developing ROI masks), so the 'automated' term as applied to quantitative neuroimaging is a bit of a misnomer.

With the development of image-analysis algorithms that took advantage of WM-GM-CSF boundary distinctions and the overall typical landmark identification of brain structure, image quantification methods became even more automated. For example, oversimplifying because of space limitations, with the introduction of a technique known as voxel-based morphometry (VBM) more automated methods for image quantification became possible (Ashburner and Friston 2000). Given the gray-scale composition of the MR image and capitalizing on the natural GM, WM and CSF compartmentalization of the brain, each designated voxel may be classified as GM, WM or CSF. If the MR image of the brain is then normalized in three-dimensional (3-D) space, such as with Talairach or Montreal Neurological Institute (MNI) coordinates (see Chau and McIntosh 2005), all similar voxels will be lined up within a uniform 3D matrix. This in turn

**Fig. 5** (Top Left) Coronal slice of original T1 weighted image at the level of the amygdala-hippocampal region. (Bottom Left) Skull stripped and intensity normalized coronal T1 weighted image derived from the original image, as shown in the top left. (Top Right) The segmented white matter estimate *wm.mgz* file created during the FreeSurfer pipeline. (Bottom Right) Subcortical and cortical segmentations overlaid onto a T1 weighted image. Note that through this method the major regions of interest and brain nuclei may be identified and quantified



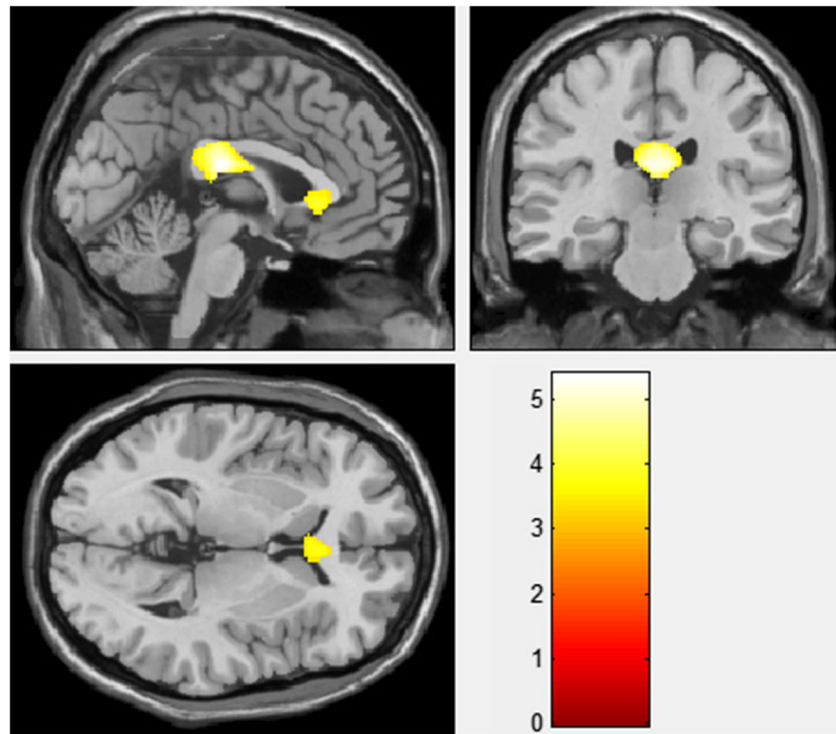
means that the local concentration of GM, WM or CSF differences between two groups within specified voxels may be established at all levels of the brain. If, for example, atrophy within an ROI has occurred, greater concentration of CSF will appear in conjunction with decreased WM or GM concentrations. Knowing the relative difference in tissue concentration across all brain voxels provides an automated localization and quantitative method showing the difference between two groups and where those differences occur in the brain. An example of this is presented in Fig. 6 that shows reduced VBM-identified WM concentration within the anterior and posterior regions of the corpus callosum in a pediatric TBI sample (image adapted from Bigler et al. 2013). Provided that there are regionally robust parenchymal changes and that all images have been properly registered and aligned, if there are voxel differences between contrasting groups or related to a particular variable, the VBM method can be an excellent one for neuropsychological investigations.

There are many variations of these techniques for structural imaging where VBM, or voxelwise analyses, represent excellent methods for coarse group comparisons (Toga 2015). For disorders like Alzheimer's disease where there are more uniform changes in GM, VBM techniques nicely capture the pathology. Furthermore, these techniques not only permit a structural imaging comparison between two groups, but a cognitive or behavioral variable may also be one of the contrasts to explore regions of difference potentially associated with a neurobehavioral or neurocognitive variable. A limitation, however comes when the pathological or developmental abnormality is very heterogeneous, more subtle and/or when pathologies do not necessarily overlap. Because of the multiple comparisons across numerous voxels any group-wise

differences have to be quite substantial and robust to survive statistical correction.

These automated methods are not without limitation, where the human eye and tracing may provide the most accurate method for ROI quantification, especially for very specific ROIs. For example, Kennedy et al. (2009) suggest that VBM techniques provide a reasonable “first pass” for determination of where differences may reside between two groups, but manual tracing of specific ROIs may provide the most accurate quantitative measurements (also see Wilke et al. 2011). Relatedly, Wenger et al. (2014) have shown that in younger healthy control, typically developing individuals (20–30 years of age) where there would be minimal age related differences and reduced likelihood of underlying pathology that automated methods approximate manual tracing. However, in older individuals (60–70 years of age) where age-related atrophy and potential for microvascular disease increases as well as other pathological changes that automated methods do less well. This is likely because with atrophy the typical delineation of gray, white and CSF boundaries sometimes becomes less well defined and irregular. Wegner et al. suggest that caution be used with older age groups in interpreting automated segmentation findings used in quantitative analyses. This cautionary note is also registered by Clerx et al. (2015). Furthermore, automated imaging analysis output of identical digital MR data may differ depending on the operating system used to run the program (Gronenschild et al. 2012). When comparing studies and findings it remains critical that attention be directed to matters related to sample size, degree of smoothing and image modulation to keep false positive rates low (Scarpazza et al. 2015). So automated methods provide great opportunity to assess large datasets

**Fig. 6** Voxel-based morphometry (VBM) comparing a pediatric TBI sample with an age and sex matched OI control sample demonstrating reduced WM at the level of the anterior and posterior corpus callosum (Bigler et al. 2013). The VBM method is highly dependent upon proper image registration and smoothing, but as shown in this illustration has the ability to demonstrate where significant differences reside related to pathological changes from trauma



but still require operator input and vigilance with regards to quality assurance and, to date, unresolved issues remain that relate to generalizability of findings across different acquisition sites and MR platforms (Chalavi et al. 2012; Diaz-de-Grenet et al. 2014; Durand-Dubief et al. 2012; Liem et al. 2015; Nakamura et al. 2014).

As already alluded to, another limitation with automated methods comes with the heterogeneity of lesions when lesion location is infrequent across a sample, variable in size and/or tends to not overlap. Without consistent pathology producing some level of uniform change in brain structure, automated techniques under detect abnormalities. This has been demonstrated by Bigler et al. (2013). As shown in Fig. 6 from Bigler et al., robust VBM differences emerged within the corpus callosum in this pediatric TBI sample. However, if just the mild TBI participants (Glasgow Coma Scale  $\geq 13$ ) with distinctly identifiable pathology as shown in Fig. 7 are examined with VBM technique, no consistent VBM difference emerges when contrasted with orthopedically injured (OI) children of similar age, education, and sex. Figure 7 shows that the abnormalities were widely distributed and did not overlap. Although the majority had regional areas of parenchymal damage, without overlapping consistent changes combined with the necessary family-wise error correction, no GM or WM areas exhibited VBM differences, including regions involving the corpus callosum. Inspection of Fig. 7 also shows that some of the pathologies were only detected on MR sequences other than the T1-weighted image, which was used for the VBM analysis. A variety of lesion-mapping techniques

applied to these data do reveal the frontotemporal preponderance of pathology and likewise, lesion volume and lesion burden metrics can be assessed. More will be said about this in sections that follow. Figure 7 is presented as a demonstration of how pathology can be below detection with VBM.

Another major improvement in quantitative structural image analysis came with the development of FreeSurfer and its public availability (Dale et al. 1999; Fischl 2012; Makris et al. 2006). Oversimplifying, basically this technique capitalizes on the gray-white-CSF segmented image and the typicality of normal brain anatomy where brain regions may be ‘parcellated’ into commonly identified anatomical regions using automated classification routines (see Fig. 5). With known boundaries and configurations for different established algorithms for different brain structures, the FreeSurfer program yields a variety of important brain metrics as well as a means to display these findings. Fischl (2012) describes Freesurfer as “...a suite of tools for the analysis of neuroimaging data that provides an array of algorithms to quantify the functional, connectional and structural properties of the human brain. It has evolved from a package primarily aimed at generating surface representations of the cerebral cortex into one that automatically creates models of most macroscopically visible structures in the human brain given any reasonable T1-weighted input image. It is freely available, runs on a wide variety of hardware and software platforms, and is open source (p. 774).”

For example, as was depicted in Fig. 5, the coronal image of the brain at the level of the hippocampus shows a typical

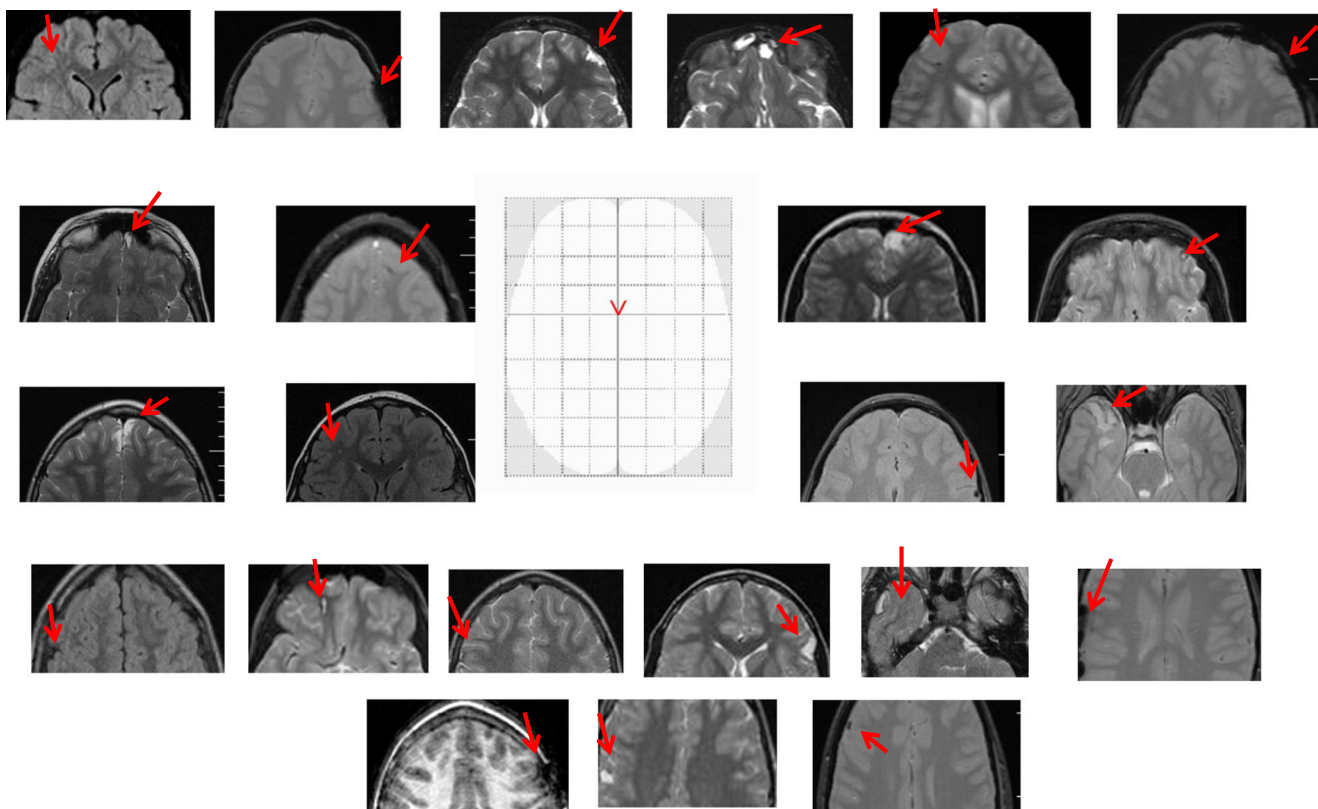


**Fig. 7** Red arrows point to where focal trauma-related abnormalities were identified in axial MR views showing a wide dispersion of lesions from children with mild TBI (see Bigler et al. 2013). Because the lesions

do not overlap nor produce any type of uniform or localized WM, GM and/or CSF differences, there no resulting significant VBM findings

parcellation with each major structure classified and color-coded. This was all done with the automated FreeSurfer program. Since the “gold-standard” for image quantification came by having neuroanatomy experts trace structures and ROIs (Good et al. 2001, 2002), these automated methods have been shown to approximate the operator controlled gold standard (Bigler et al. 2010), but the same limitations as described above for any voxel-based technique still apply. Furthermore, FreeSurfer results are highly reproducible. Hand tracing of major brain structures and ROI analyses could take over 100 h per scan whereas the images presented in Fig. 5 and the corresponding quantification was achieved in a matter of minutes to hours, once properly formatted. For any FreeSurfer ROI a volume or other quantitative metrics may be computed (Figs. 5, 8, 9 and 10 all show the utility of the FreeSurfer method).

In viewing Fig. 5 the cortical ribbon of gray matter runs along the entire surface of the brain. Cortical thickness has implications not only for developmental stage of any cortical region in terms of thickness and volume but also for injury. FreeSurfer provides a method for surface definition classifying the brain by gyral or Brodmann areas (Desikan et al. 2006; Destrieux et al. 2010). For each ROI, volume may be calculated or within FreeSurfer’s Query, Design, Estimate, Contrast (QDEC) function cortical thickness, cortical volume or pial surface (a method to estimate gyration) computations may be calculated and examined in

the context of a neuropsychological variable. Figure 8 is the author’s FreeSurfer derived 3-D brain showing the cortical

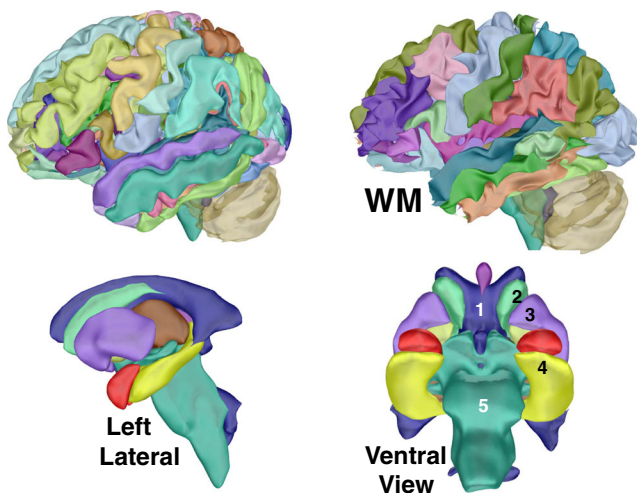
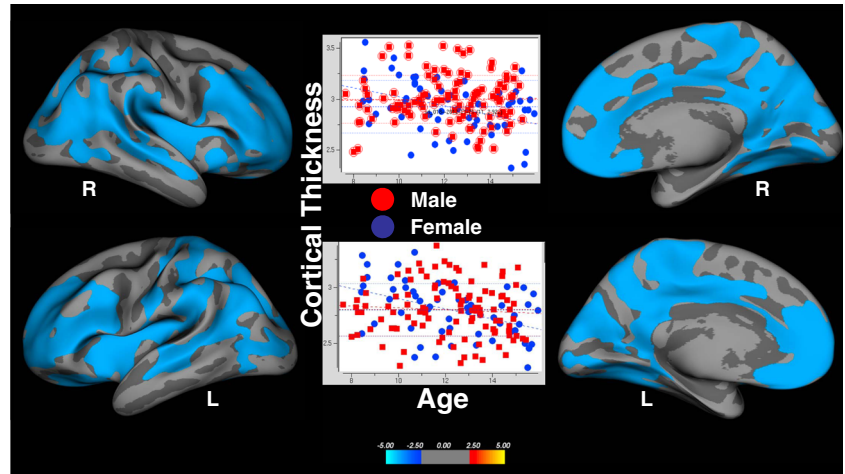


**Fig. 8** Derived from the T1-weighted image shown in Fig. 1 (right side), the FreeSurfer analysis that extracts gyral volume (upper left) and WM volume only (upper right) are presented. Similarly derived from FreeSurfer, left lateral and ventral views of subcortical structures where the following colors identify the following: (1) Blue –lateral ventricle, Above 1: purple corpus callosum, (2) aquamarine – caudate, (3) purple – putamen, (4) yellow – hippocampus, red above 4: amygdala. 5- pons/brainstem. Volumes and other metrics may be derived from each color coded region

**Fig. 9** Query, Design, Estimate, Contrast (QDEC) analyses demonstrating regions (in blue) where reduced cortical thickness occurs with increased age. Scatter plots are presented for the right (R) and left (L) hemispheres. Age range from 7 to 16 years of age. See Fig. 10



surface colorized to identify different cortical gyri from which gyral volume may be calculated. Also shown is the appearance of WM cortical volume. Since WM is situated beneath the cortical mantle, it has a much thinner appearance than the gyral volume and surface area. Furthermore, Fig. 8 also depicts subcortical ROIs and the brainstem as depicted in 3D. Accordingly, a variety of ROIs and metrics may be computed using these techniques, including regional volumes, cortical thickness, and surface area (Rimol et al. 2012).

The FreeSurfer technique, and other methods like it (see Toga 2015) is useful for examining contrasts between two groups or to examine the influence of a particularly meaningful variable, like age. For example, using the FreeSurfer method Fig. 9 shows an overall reduction in cortical thickness with age from 7 to 16, inferred from cross-sectional data and thought to reflect neuronal pruning associated with maturation (Stiles and Jernigan 2010). Returning to the pediatric TBI study introduced as part of Fig. 6, but now examining brain relations to a cognitive variable

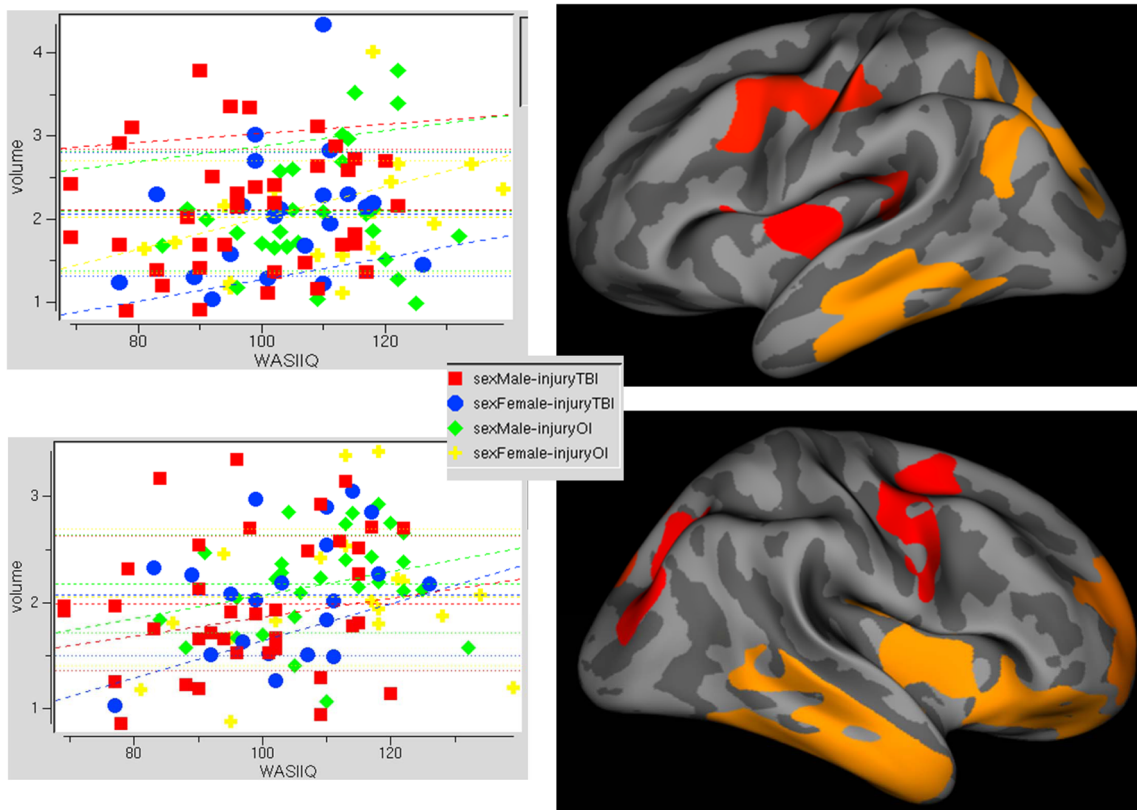


**Fig. 10** Query, Design, Estimate, Contrast (QDEC) analyses of the relation between the left hemisphere (*Top*) and right hemisphere (*Bottom*) cortical volume with level of intellectual functioning (Full Scale IQ as

measured by the Wechsler Abbreviated Scale of Intelligence (WASI, Wechsler 1999) in a combined sample of TBI and OI subjects where age and sex were controlled

controlling for age, to correct for the age-dependent changes shown in Fig. 9, the relation of cortical volume to intellectual ability in this sample is presented in Fig. 10. As observed in Fig. 10, there is a positive correlation between regions of cortical volume and intellectual ability. Using techniques like FreeSurfer, just about any cognitive or neurobehavioral variable may be explored in relation to structural brain imaging findings.

Despite the straightforwardness in setting up the statistical contrasts for FreeSurfer and other image analysis programs, as Fama and Sullivan (2014) point out it remains important to establish whether a particular brain region or neural network reliably relate to a neuropsychological variable. Fama and Sullivan recommend various association and dissociation methods including the “double dissociation” methods used by Teuber more than half a century ago, which still apply to contemporary image analysis (see Teuber 2009, this is a reprint of his 1964 classic paper that used the double dissociation method to differentiate the neuropsychological effects of frontal versus posterior lesions). An excellent example of this comes from the study by Krueger et al. (2011) where they used FreeSurfer to derive ROI frontal volumes in a large group of individuals with a mixture of various neurodegenerative diseases. The double dissociation they set up and hypothesis tested was that regions of the dorsal lateral prefrontal cortex (DLPFC) would be more related to executive functioning in contrast to the orbitofrontal cortex (OFC), which would relate more to socioemotional disinhibition. These investigators were able to establish a “double dissociation” where in fact DLPFC volume predicted performance on executive function tasks but not on tasks of emotional disinhibition, with the reverse observed for OFC. As Fama and Sullivan indicate, the double dissociation method represents a “gold standard” for use in these kinds of neuroimaging-neuropsychology analyses where complex associations are being determined.

A particular advantage for neuropsychological research is that automated image analysis techniques using FreeSurfer as well as similar measures are being used to apply a uniform quantitative assessment metric to large datasets (Fischl 2012; Tustison et al. 2014). In the past, a criticism of neuropsychological research has involved sample size issues and being statistically underpowered for the hypothesis being investigated (Levin 1997; Millis 2003). With these neuroimaging advances like FreeSurfer, such methods have the potential to provide normative neuroanatomical as well as neuropathological data for neuropsychological function and outcome studies across all neurological and neuropsychiatric disorders. At the individual subject level this means that in the future known structural neuroimaging values will be available for any individual undergoing neuropsychological examination provided that the proper MRI studies have been performed. Nonetheless, as already alluded to major issues still require resolution when using FreeSurfer including how variations in image acquisition influence results as well as how different MR platforms influence analyses, along with day-to-day variations that can occur in the same subject.

Figure 11 illustrates how slight alteration in the image sequence acquisition and different image platforms influence FreeSurfer output. The boundaries for segmentation and classification, as was shown in Fig. 5 depend on WM-GM-CSF differentiation which in turn is dependent on signal intensity. In Fig. 11 the fidelity of signal intensity is compared across a gray scale range comparing two scans run separately under differing conditions. In the top if the identical scan from the same individual is run separately, perfect fidelity in signal intensity is achieved along with identical FreeSurfer output. This demonstrates the reproducibility of FreeSurfer findings based on separate analyses of the same data. However, the middle image in Fig. 11 is from the same individual but now scanned on two separate occasions with a slight difference in image acquisition parameters. Note that fidelity remains good but not perfect. Lastly, if MRI data is obtained on different days and different platform there is even less fidelity, although remains highly correlated. In both the middle and bottom figures the FreeSurfer output differed.

To better quantify these issues, Iscan et al. (2015) examined 40 healthy controls who were scanned twice on the same scanner and then a subset of 10 subjects who traveled and examined on two different scanners. They also used a visual inspection rule to “disapprove” where segmentation/parcellation errors may be apparent. For those scanned twice on the same scanner intraclass coefficients where all high ( $>0.8$ ) and percent difference all low (one percent or less). However, including those who did not pass visual inspection or scanned on two different scanners yielded higher variability.

Streitburger et al. (2012) used FreeSurfer to demonstrate another potential source of variability in volumetric computation. Healthy volunteers underwent MRI during normal hydration, hyperhydration and dehydration. The dehydration condition resulted in significant decrease in both WM and GM volumes. In longitudinal studies given the multiple factors mentioned above suggests that any normative database using FreeSurfer or related measures (Ochs et al. 2015), will have to consider that there will just be a certain amount of variance that just cannot be fully controlled.

The examples shown thus far for automated image analyses have been mainly discussed in terms of whole brain analyses, but analyses may also be directed to a specific region, when for example there is an *a priori* hypothesis for a particular ROI, like the basal ganglia, cerebellum or hippocampus (Glatz et al. 2015; Suppa et al. 2015; Wu et al. 2012). In such circumstances a “mask” is placed over the ROI, so that comparisons are focused just within the ROI, reducing some of the restrictiveness of family wise error.

## MRI Structural Imaging Basics

This review began with an immersion in various image quantification methods and their historical root. However, all

### Voxel-by-Voxel Signal Intensity Under Different Image Acquisitions

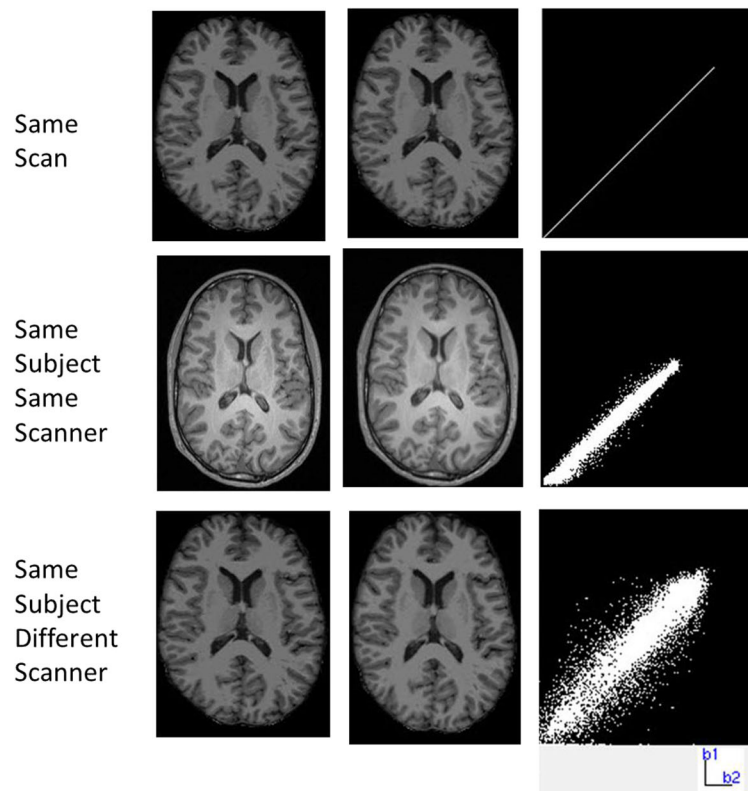


**Fig. 11** Voxel-by-voxel signal intensity under different image acquisitions. Subtle differences in image acquisition and even scanning the same individual but on different scanners has the potential to yield different results. b1 (y-axis) refers to the first scan shown on the left and b2 (x-axis) refers to the second scan, as shown on the right. The plots to the right reflect the distribution of signal intensities values for the different b1-b2 comparisons. (TOP) This is from the same individual with the same scan run twice. As expected, perfect fidelity. (MIDDLE) This is from a different subject than shown in the top images, but this individual is assessed on the same scanner on the same day two times, with the

second acquisition slightly different. Note good but not perfect fidelity in the distribution of signal intensity findings even though the images appear similar. (BOTTOM) This is the same individual as shown in the top illustration but this time scanned on two different platforms with similar acquisition sequences separated by approximately a month. Note these kinds of differences yield the greatest variation in signal intensity findings. The point with this illustration is that differences in the acquisition sequence and/or platform even in the same individual results in some variability

structural imaging techniques originate with the scan image itself and whether a clinician or researcher, a foundation in MR basics is important. There are numerous excellent texts on this topic, for example, Hashemi and Bradley (2010), with the next section providing some highlights.

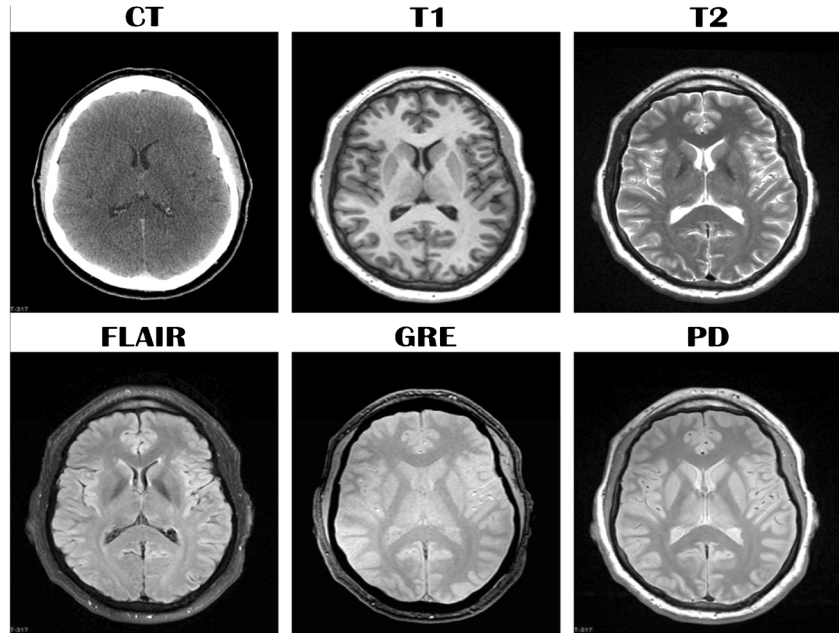
### MRI Basics

There is much written on the fundamentals of MR imaging and clinical application for identifying brain structure (Bitar et al. 2006; Plewes and Kucharczyk 2012; Rosenbloom et al. 2003; Sullivan and Pfefferbaum 2007; Wilde et al. 2014). In brief, the image of the brain derived from MR scanning reflects electromagnetic signal intensities from hydrogen nuclei as displayed on a gray scale. The resonance interaction between hydrogen nuclei and externally-applied magnetic fields generates the MR signal, which in turn, is spatially encoded to provide a mapping of imaged areas. Signal intensity depends on the magnetic

environment and hydrogen nuclei density (i.e., protons in water) that differs by tissue types. WM, GM and CSF all have characteristic MR signals that differ one from the other (Fig. 12). Depending on the MR sequence different tissues are characterized by their signal intensity, appearing brighter or darker on the images as reflected in the standard MRI sequences shown in Fig. 12. Accordingly in MR parlance, the signal is described either as being “hyperintense,” “isointense,” or “hypointense.” For comparison, in the same subject, Fig. 12 also depicts an axial CT scan at the same level as the MR sequences. However, the CT brain image is based on a tissue density function derived from the x-ray beam passing through brain parenchyma.

The use of innovative methods for varying magnetic field strength, different types of head coils, the delays between sending and receiving electromagnetic waves, and the acquisition and display of the signal intensity allow the production of a range of images, some of which best demonstrate anatomy while others are more useful in detecting specific forms of pathology. For

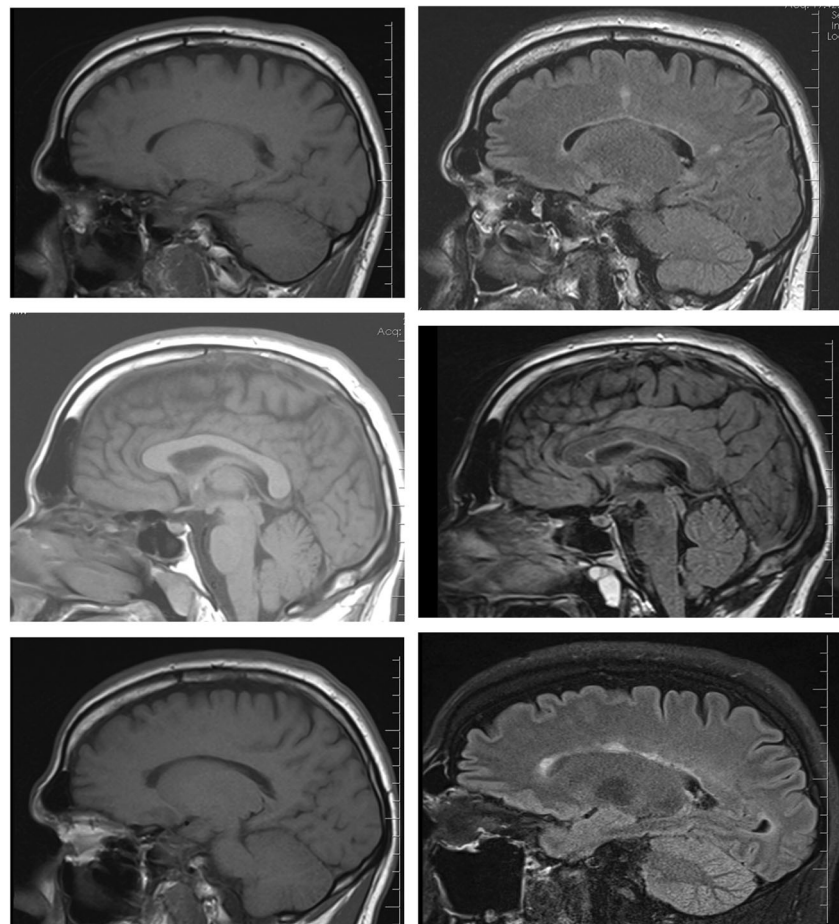
**Fig. 12** Comparison of computed tomography (CT) and several different MRI axial views at the same level. Fluid attenuated inversion recovery (FLAIR), gradient recalled echo (GRE) and proton density (PD) sequences are shown on the bottom row. Note the symmetry regardless of the sequence and how the left hemisphere mirrors the right



example, T1-weighted images tend to show excellent anatomical detail, but may not differentiate certain forms of pathology because they are less sensitive to signal from CSF or to differences in adjacent tissue signal between what may be normal or

abnormal. For this reason the T1-weighted sequence is the most commonly used structural MR method for defining neuroanatomy and automated image quantification. A common problem with pathology detection using T1 imaging is shown in Fig. 13

**Fig. 13** This patient has multiple sclerosis (MS); however, the white matter abnormalities characteristic of MS are not distinctly detected on the T1-weighted sequence (*left column*), whereas white matter hyperintensities (WMHs) are readily observed in the fluid attenuated inversion recovery (FLAIR) sequence (*right column*) that are at approximately the same level. (*Top, left and right*) Left hemisphere, (*Middle, left and right*) Mid-sagittal and (*Bottom, left and right*) Right hemisphere. Note that there is some subtle signal difference in the T1-weighted images where the most prominent FLAIR abnormalities were located



in a patient with multiple sclerosis. The sagittal T1 images of the corpus callosum at midsagittal level and on either side generally appear normal in size, configuration and signal intensity on the T1. However, similar levels with imaging from a sagittal fluid attenuated inversion recovery (FLAIR) sequence shows the characteristic white matter hyperintensities (WMHs) of demyelinating disorder. T2-weighted images, which are particularly sensitive in detailing CSF, generally show normal structures as having an intermediate (gray) intensity, while fluid and many pathologic abnormalities appear with high intensity (white), often providing the kind of contrast between normal and abnormal tissue types indicative of pathology (this will be shown in some of the figures that follow). Other sequences that provide averages of T1- and T2-weighting are called mixed, balanced or proton density (PD) sequences. Common appearances of typical tissues on MRI are listed in Table 1.

The gradient (recalled) echo (GRE) affords good image detail with short imaging times and is sensitive to the presence of blood and a blood breakdown product referred to as hemosiderin. Hemosiderin (principally iron from blood) presence within brain parenchyma is reflected as a hypointense or dark signal especially notable as a residual from prior hemorrhage in the region detected. Presence of hemosiderin in brain parenchyma can also suggest the presence of neurodegenerative changes such as gliosis in surrounding tissue. Susceptibility-weighted imaging (SWI) utilizes a different GRE pulse sequence which is particularly sensitive in detecting residual hemorrhages within brain parenchyma, which appear as hypointense (dark) regions. Figure 14 shows a case with SWI and FLAIR along with T1, T2 and PD-weighted images in a patient with TBI, where the presence of these two abnormalities likely reflect gliotic tissue and extensive white matter pathology as well. Note that each image sequence reflects different qualities of the underlying parenchymal damage from trauma.

The colorized lesion map in Fig. 14 outlines a major problem for neuropsychology when it comes to defining lesion analysis, because each MR sequence provides unique information about brain structure. Accordingly, depending on which image sequence is used, different pathological characteristics may be highlighted. For example, using the FLAIR sequence prominent regions of WMH may be isolated but note these abnormalities are different than where the focal hemorrhagic lesions are located, or where focal encephalomalacia has developed. Accordingly, either quantifications of focal lesion burden by pathology category can be computed or summed to produce an overall index of lesion burden. Also, abnormalities can be anatomically disparate. The diversity of lesion localization, lateralization, and presentation adds to the challenges in defining what and where abnormalities may reside that may be relevant to neuropsychological outcome.

## Interpretative Guidelines for Structural Imaging Analysis in Neuropsychology

There is still much to be gained by examining the gross anatomical structure of the brain and for disorders where the pathology is not subtle, the clinical reading of structural imaging findings correlated with neurobehavioral features may provide great insights to behavioral-brain relations in neuropsychology. Along these lines the section that follows provides interpretive insights for neuropsychology based on structural imaging findings when neuroimaging is available for review.

### Similarity Principle

Normal brains have a typical shared appearance although individual differences will specify that no two brains are exactly

**Table 1** MRI appearance of commonly scanned tissues

Tissue	T1-weighted	T2-weighted GRE	T2-weighted FLAIR
Gray matter	Gray	Light gray	White/light gray
White matter	White	Dark gray	Dark gray
CSF or water	Black	White	Black
Blood	Depends on timing (white – gray)	Black with blooming	Black without blooming
Fat	White	Black	Black
Air	Black	Black	Black
Bone or calcification	Black	Black	Black
Edema (established)	Gray	White	White
Demyelination or gliosis	Gray-black	White	White
Ferritin deposits	Dark gray	Black	Black
Calcium bound to protein	White	Dark gray	Dark gray
Proteinaceous fluid	White	Variable	Variable

On fast spin echo (FSE) sequences (a faster variant of the SE sequence), fat appears bright in T2-weighted. Blooming=amplification of the lesion

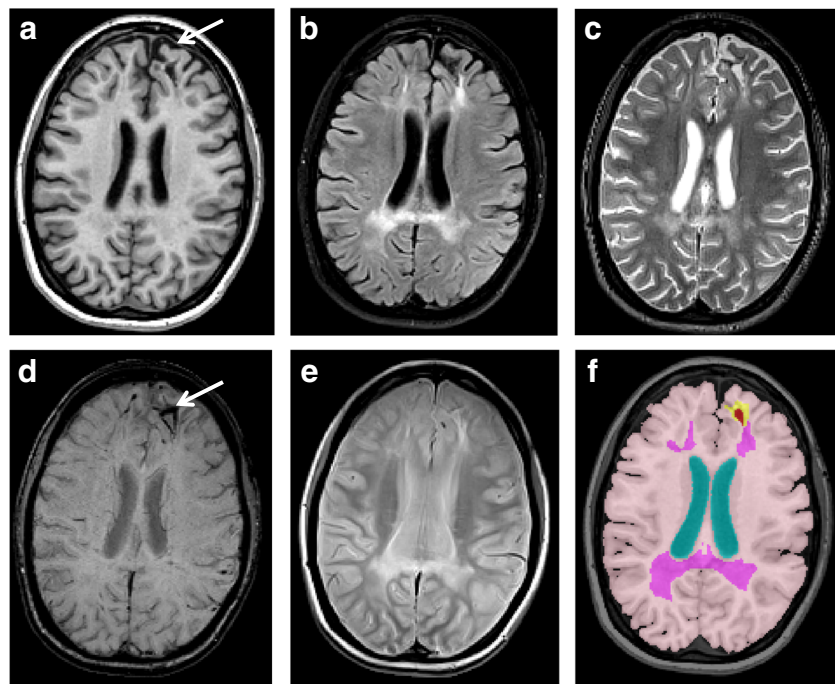


**Fig. 14** This is case of severe TBI with MRI studies obtained during the chronic phase (>2 years post-injury), with all axial images at approximately the same level. **a** T1-weighted image with arrow pointing to focal frontal atrophy. **b** Fluid attenuated inversion recovery (FLAIR) sequence that shows extensive white matter signal hyperintensity (WMH). **c** T2-weighted image where the white matter signal abnormalities are not as robust as with the FLAIR, but still observable. **d** Susceptibility weighted imaging (SWI) sequence with prominent frontal (white arrow) hemosiderin deposition. There are other regions of scattered hemosiderin deposition (hypointense dark signal), but none as large as in the frontal lobe. Returning to the T2 image in C, note that hemosiderin is

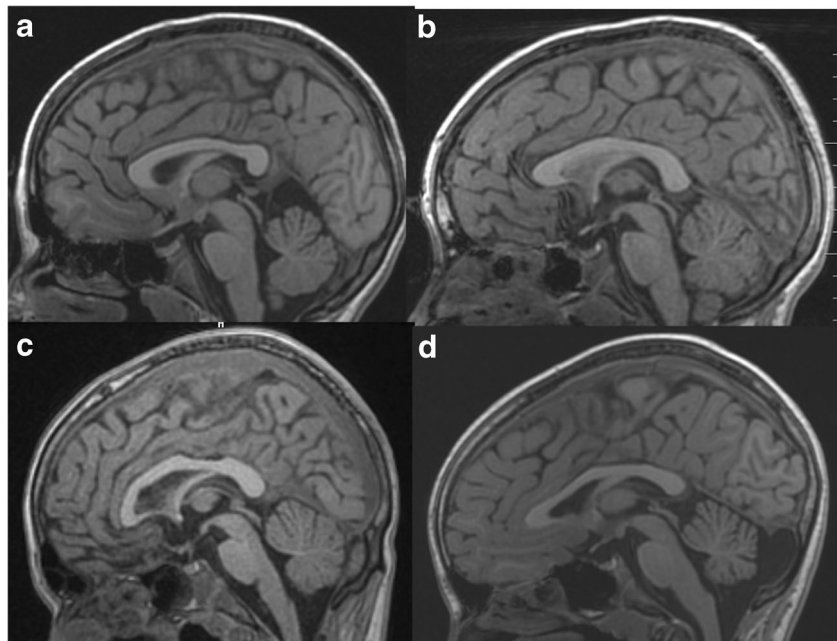
detected as well, although limited. **e** Proton density (PD) which also demonstrates the white matter hyperintensities. **f** The color map highlights the isolated WMHs in pink, ventricle in aquamarine; the red-yellow reflects the centrality of the primary location of the largest region of hemosiderin in the frontal lobe in combination with focal parenchyma changes. Given the diversity of abnormalities, which color-coded region used for image analysis may differentially relate to neuropsychological outcome. For example, total white matter lesion burden and speed of processing appears to be an effective comparison for establishing post-injury neuropsychological outcome (Delano-Wood et al. 2009)

alike. Returning to Fig. 1, even though one is a photograph of a post-mortem brain and the other the author's gray-scale depiction from MRI, they both appear similar and recognizable like any other brain cut in the coronal plane at this level. Figure 15 demonstrates this principle in another way by comparing four mid-sagittal T1-weighted images of four different individuals. In each, MRI scan identification of the corpus callosum from four different children, 12 to 16 years of age is straightforward by its distinct elongated appearance and WM signal. Two are males and two female. One male and one female adolescent are from an orthopedically injured (OI) control group not meeting any criteria for having sustained a head injury, but meeting criteria for being typically developed other than having sustained an upper or lower extremity fracture. By contrast, there are two who sustained a TBI. Is there anything in the image that distinguishes the two cases with TBI? Likewise, is there something that distinguishes the male from the female brain regardless of whether injured or not, or who is the 12 year old versus the one who is 16? Because of the 'similarity principle' the corpus callosum, and the rest of the mid-sagittal

appearance of the brain, has a similar appearance and location across all four brains, regardless of male or female or age. Although corpus callosum shape is different and unique for each individual, the signature general appearance of an elongated WM structure located at midline is unmistakable. Corpora callosa are similar in appearance. Likewise, the same is true for every other region examined, including gyral and cortical patterns as shown in Fig. 15. However, despite the recognizable features at this level of gross visual analysis, there is nothing that permits distinguishing who might be male or female. With regard to injury, the bottom scans are from the brain injured subjects. Careful visual inspection does imply some reduction in corpus callosum size when compared with their OI control counterparts, although possessing small corpus callosum size is not conclusive for or diagnostic of TBI. Some of these differences may be more definitively illuminated with quantitative analyses of the structural images of the brain, as will be shown for the case depicted in Fig. 15c.

As presented in Fig. 16, a large frontal defect is readily visible and identifiable regardless of the image sequence but

**Fig. 15** Four mid-sagittal T1-weighted images are presented highlighting the similarity principle showing general and similar appearance of the corpus callosum and mid-sagittal area of the brain across all four subjects. The top two are female (**a**) and male (**b**) orthopedically injured compared to male (**c**) and female (**d**) TBI research participants. On closer inspection, the corpora callosa while distinctly recognizable as the corpus callosum in each subject appears thinner in the bottom two images in the TBI patients. Atrophy of the corpus callosum is a characteristic feature of TBI. There is no visibly detectable method for identifying male/female differences of the brain



especially prominent in the T2 and FLAIR images. While all of these images reflect a brain the defect violates the similarity principle, because age-typical healthy brains do not have abrupt signal differences like this within the parenchyma (compare the same MR image sequences from the injured brain in Fig. 16 to the healthy control brain in Fig. 12). Note that regardless of the image sequence outside of where the lesion is located, the transitions between predominantly GM, WM and CSF tissue types follow well defined boundaries with even transitions in the non-focally damaged parenchyma. By contrast, around the focal frontal lobe lesion the signal differences are irregular with abrupt demarcations, depending on the imaging sequence, in violation of the “similarity principle” and thereby defining a region of abnormal tissue.

### Symmetry Principle

Returning to Fig. 12, from a healthy typical developed adult individual, regardless of the image sequence the distinct symmetry of how one hemisphere mirrors the other represents another readily apparent and visualized characteristic of the healthy brain. The age-typical healthy brain is grossly symmetric, regardless of the imaging plane (see Figs. 1, 5 and 8). This also means that in the study of lateralized injury or damage, such as that from trauma, stroke, infection or focal neoplasm, the unaffected hemisphere may be used for comparison, both qualitatively and quantitatively. In this manner each patient may serve as their own control. This is also shown in Fig. 16 of the frontal damage in the case presented therein. Comparing the side with damage to the other hemisphere

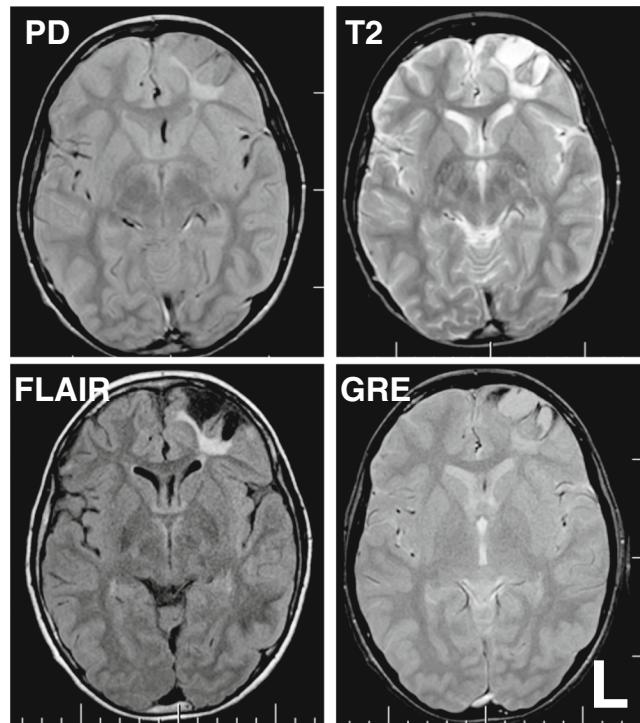


**Fig. 16** This is the same subject as shown in Fig. 15 (C, lower left) who sustained a severe TBI. There is a distinct large defect, essentially a divot that has been created by the severe TBI and multiple, scattered hemorrhagic contusions that occurred in the original injury (see Fig. 17). The four axial images depict different features of the pathology. Note how the *FLAIR* images denote the loss of brain parenchyma but just underneath the prominent focal frontal defect are areas of hyperintense signal in the WM. Images are in radiological perspective, with left (L) on the viewer's right

where no gross damage is present straightforwardly demonstrates differences, violating the symmetry principle.

### Size-Normalcy Principle

The bilaterally symmetric regional components that form a healthy brain develop within a normalcy principle. An anatomical example of this developmental principle may be visualized by plotting some aspect of brain development over time, as was shown in Fig. 9. Viewing the scatter plot that depicts cortical thickness in Fig. 9, a range of normalcy is displayed. While there will always be a few outliers, two observations are evident in these plots: (1) most individuals have total cortical thickness that congregates within a range of expected values but (2) varies with age. Having a sample of individuals with typical development at a given age permits comparison with a target clinical sample where deviations from the normalcy principle suggests aberrant development and/or, depending on the disorder being examined, pathological consequences (i.e., atrophy) of some disease, trauma or disorder. Because disorders varying by age, time since onset, whether focal, multifocal or disseminated, there are numerous factors that require consideration. The importance of the size of a structure is relevant for its function, as described next.

### Size-Function Rule

Within the broad field of biology, allometry is defined as the study of body size in comparison to shape, anatomy, physiology and behavior with the assumption that certain body characteristics evolved to fit a particular function. At a basic level there exists some relation of anatomical size to the function subserved by that brain region. An excellent example is olfaction. Comparative neuroanatomy shows that in humans, the olfactory bulb in proportion to overall brain size is minuscule in contrast to the proportionally large olfactory bulb in the canine or other mammals that depend on smell (Schmidt et al. 2012a; Stephan et al. 1987). Nonetheless, in humans the size of the olfactory bulb relates to the accuracy of olfactory discrimination (Buschhuter et al. 2008; Haehner et al. 2008), developmental improvements in olfactory discrimination with maturation (Hummel et al. 2011) and proportional size evolutionary changes in primates (Barton 2006). Indeed there is even plasticity with enhanced olfactory functioning and discrimination ability associated with olfactory bulb volume in those with early blindness (Rombaux et al. 2010). Sensory loss in one system becomes the plasticity trigger to enhance function within other sensory modalities and this is mediated by volumetric changes in the target structure.

At least at coarse levels of analysis, this size-function rule applies to domains of cognitive functioning, clinical disorder and neural networks. For example, abnormally small volume

in the anterior cingulate and dorsal lateral prefrontal cortex, known areas that are part of executive control and the default-mode network thought to be aberrant in attention-deficit/hyperactivity disorder (ADHD), are reduced in size in ADHD (Kessler et al. 2014). As first shown by Willerman et al. (1991) a positive correlation exists between overall brain volume and intellectual ability, replicated by numerous studies (see Lange et al. 2010; Luders et al. 2009; Toga and Thompson 2005). These positive correlations between brain volume and IQ also can be demonstrated with cortical volume, as was shown in Fig. 10. Interestingly, there is also a positive relation between brain size and connectivity (Hanggi et al. 2014). If IQ coarsely relates to brain volume, it does mean that when substantial IQ differences between contrasting samples are present, the IQ-brain volume issue needs to be addressed in the design of the study or statistical analysis.

**Goldilocks Principle** If the emergence of typical cognition or behavior is dependent upon particular neural systems, the coalescence of genes, development, experience (environmental exposure) and size likely result in an interactive effect producing a “just-the-right-size” scenario, matching function to size. As the fairy tale goes Goldilocks selects the porridge that is “just right.” As introduced above the overall correlation of human brain size (volume) with IQ is positive, consistently shown to hover somewhere from .2 to .5 (Lange et al. 2010; Taki et al. 2012; Toga and Thompson 2005; Willerman et al. 1991). However, as is well known in the pediatric literature brain growth that is either too small (microcephaly) or too large (macrocephaly) is associated with intellectual deficits and developmental disorders (Fombonne et al. 1999; Mirzaa and Poduri 2014; von der Hagen et al. 2014). The normalcy development as reflected in Fig. 9 reflects the “just-the-right-size” phenomena of typical brain development.

### Clinical Rating Methods

A variety of clinical rating methods are available that provide a rapid method to describe general MRI findings (Bergeson et al. 2004; Davies et al. 2009; DeCarli et al. 2007; Frisoni et al. 2003; Scheltens et al. 1993, 1995). Although much of this review has focused on a variety of brain imaging analysis techniques that provide elegant images of the brain and potential regions of pathology, all require post-processing and the proper hard and software as well as knowhow to carry out the analyses. That is not always a practical solution especially for applied research purposes, where clinical ratings provide reasonable indicators of abnormal brain structure. The methods established by Scheltens et al. are some of the most widely used for describing white matter pathology on the PD, T2-weighted or FLAIR images and have been applied to diverse types of disorders (Prins and Scheltens 2015). Some of these clinical ratings may be used for grading whole brain or

regional atrophy, including hippocampal atrophy. Quantitative metrics will continue to be the standard, but there is utility in qualitative clinical ratings.

## Applying Structural Image Analysis Tools in Neuropsychology

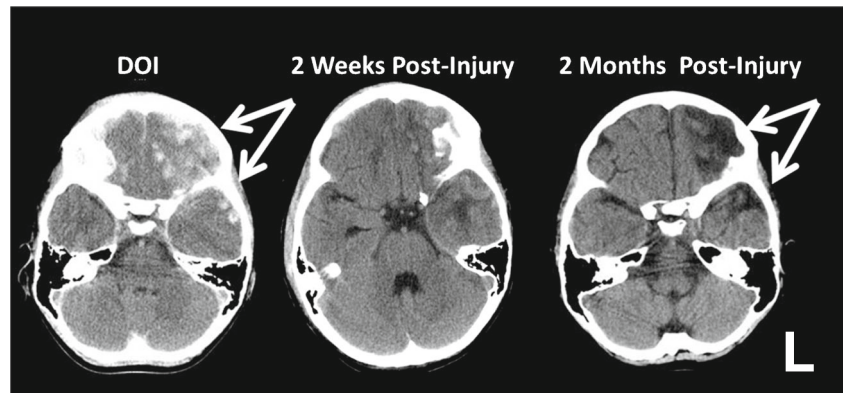
An extensive and diverse armamentarium of structural image analysis techniques now exists for the study of anatomical brain correlates of neuropsychological function (Brewer 2009; Catani et al. 2012; Cox et al. 2014; Toga 2015; Tustison et al. 2014; Wilde et al. 2012). To show some of the quantification techniques that now can be done, the TBI case with focal lesions introduced in Figs. 15c and 16 is further analyzed. However, the story of the lesions or identifiable abnormalities and what to measure is quite complex and must begin with the original injury. As will be shown, a multi-modality approach to structural imaging findings will likely be key in future neuropsychological investigations.

The day of-injury (DOI) CT scan, as shown in Fig. 17, demonstrates extensive hemorrhaging, including multiple hemorrhagic contusions that occurred in the frontal region, and less extensively in the temporal region (white arrows point to numerous hemorrhages – white splotches within the parenchyma). However, it takes weeks for stabilization of the frontal pathology to emerge as encephalomalacia, focal atrophy and loss of parenchyma. Longitudinal studies in those with TBI have shown that it takes a minimum of 6 weeks for prominent encephalomalacia consistently to be apparent in imaging studies (Blatter et al. 1995), with dynamic changes in lesion size, volume and regional atrophy extending across the first year to even longer timeframes post-injury (Farbota et al. 2012; Green et al. 2014; Ng et al. 2008). As visualized in Fig. 17, the CT images over a 2 month timeframe show dramatic changes in the appearance of the frontal lesion. If structural imaging analysis focused on the evolving lesion too early, it would likely underestimate lesion volume. Also, this illustration underscores the potential influence timing has on defining the size, shape and quantitative analyses of what a

lesion may be. Although this example is from TBI, the same principles basically apply regardless of etiology that may produce focal damage and how it changes over time.

Moving to imaging obtained definitively within a chronic timeframe, in the case of the subject presented in Figs. 15, 16 and 17 four years post-injury, lesion pathology is stable at this point but then deciding on what to measure as lesion size or volume presents several issues. Returning to Fig. 16 comparison of the PD, T2, FLAIR and GRE sequences show different aspects of brain pathology where each sequence highlights a different aspect of residual abnormalities caused by the trauma. Notice in particular that the FLAIR sequence shows cystic cavitation at the site of the prior frontal contusions viewed in the CT imaging, with complete loss of brain parenchyma and back filling of CSF. Clearly loss of tissue reflects a lesion and turning to the surface rendered 3-D image of the brain in Fig. 18 the extent of the left frontal pole damage is substantial as depicted in red, which reflects loss of brain parenchyma. The size of this lesion may be volumetrically quantified by defining regions where there remains parenchymal signal versus what is CSF (red region as shown in the left frontal lobe in Fig. 18). However, this is not the totality of the “lesion” since there is hyperintense signal within the frontal WM as shown on the FLAIR sequence (see Fig. 18 solid white arrow, bottom right axial image). There is still WM parenchyma present; however, because of the injury, and likely biomechanical deformation that has degraded WM integrity, the MR signal in WM is abnormal extending into the deep WM of the frontal lobe. As a result, the actual “lesion” volume of frontal lobe damage is substantially larger than just where the focal encephalomalacia may be visualized (again, red area as shown in Fig. 18). As shown in Fig. 16 there is also hemosiderin deposition that borders the WMH signal abnormality and encephalomalacic changes in the GRE sequence (lower right image). Thus a more accurate estimate of the focal left frontal damage would include the combined lesion boundaries from all of the MR sequences that depict abnormal signal. Figure 19 shows a lateral view of the cystic lesion (red) and the abnormal WMH behind it with the areas of hemosiderin deposition embedded within (not shown). The distinct WMH abnormalities

**Fig. 17** Day-of-injury (DOI) CT images show multiple hemorrhagic lesions in the left frontal and temporal lobe regions (arrows). By 2 weeks later much of the hemorrhage had been reabsorbed but tissue degradation is also occurring and by 2-months post-injury prominent encephalomalacia has replaced where the original intraparenchymal and surface hemorrhages occurred (arrows)



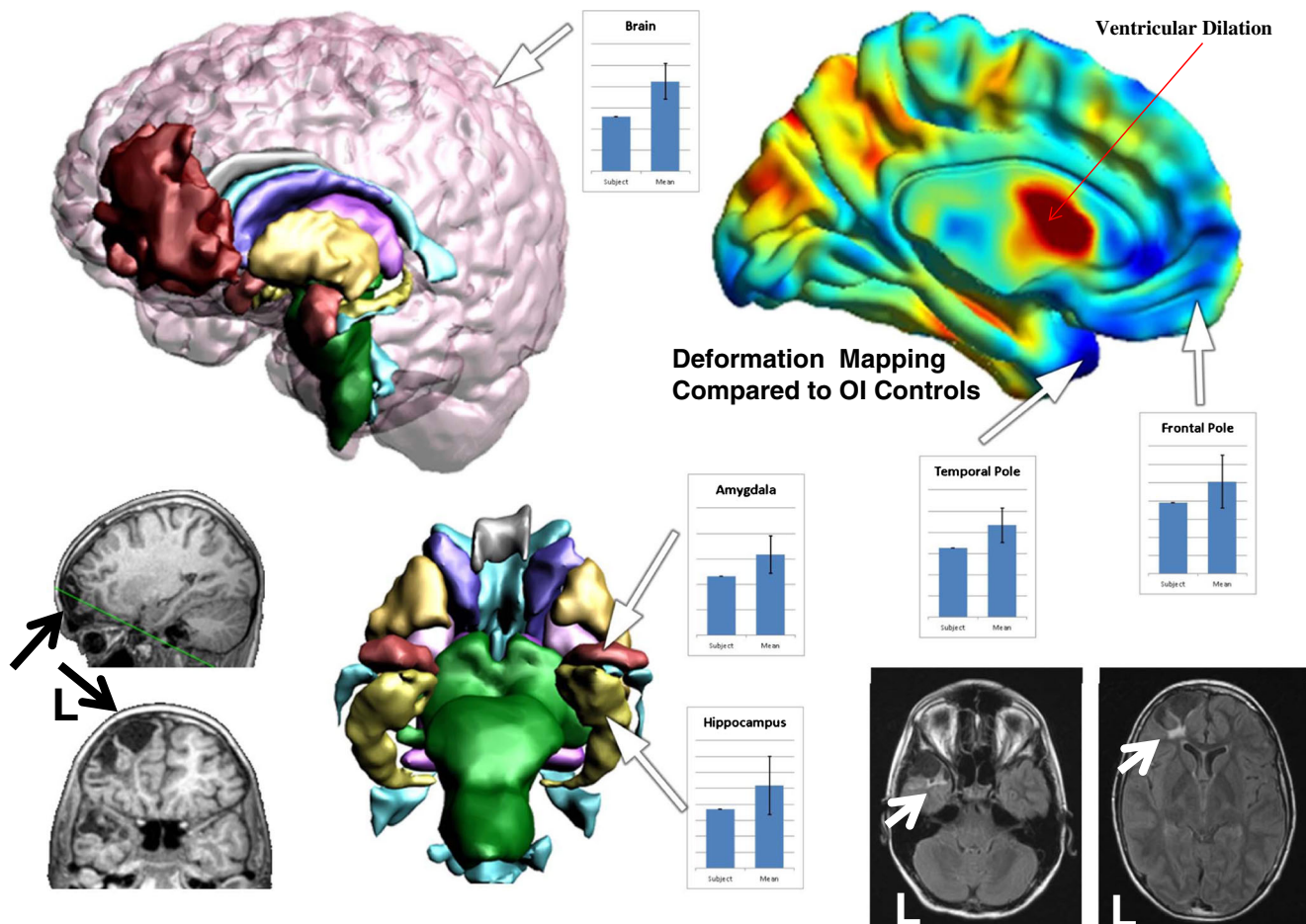


**Fig. 18** Three-dimensional (3-D) rendered image based on FreeSurfer analyses depicting the large area of focal frontal pathology. The red represents the focal area of encephalomalacia (black arrows) as depicted in the T1 images (black arrows) in the lower left (L=Left Hemisphere). The upper right image is a surface rendering from ANTs following deformation analysis comparing this individual subject to a normative dataset matched for age and sex. “Cold colors” (blue colors) reflect significant

volume reductions in contrast to “warm colors” that indicate significant increase in volume is present. Histograms are from FreeSurfer derived volumes for whole brain, amygdala, hippocampus, temporal pole and frontal pole. Note in each case a substantial and significant reduction in volume has occurred. Lower right shows the FLAIR sequence depicting both WM signal abnormalities in the frontal and temporal lobe regions (see Fig. 19) with left (L) now on the viewer’s left

required a separate type of image analysis to identify the boundaries of all significant WMHs present (see Schmidt et al. 2012b), as depicted in Fig. 19. In terms of the total left frontal lesion border, what is shown in Fig. 19 as red and aquamarine would be the most accurate.

Additionally, in this research participant the damage is not just restricted to the frontal lobe, as implicated by what is depicted in Fig. 19. So how should this multifocal to disseminated pathology be reported, especially areas where atrophic changes have occurred? One method would be to use FreeSurfer volumetric calculations of all cortical and subcortical ROIs compared to a normative sample matched in age and sex. In other words derive all of the volumes for all ROIs as presented in Figs. 5 and 8. Indeed, as shown for some select regions as depicted in Fig. 18, based on these FreeSurfer calculations, frontal and temporal polar area volume loss compared to a normative sample exceed more than a standard deviation

below the mean for typical developed individuals of similar age and sex, as did hippocampal and amygdala volume. While a bar graph presentation is straightforward for specific ROIs, potentially a much better graphic than multiple bar graphs, is what is referred to as deformation mapping of the brain showing in the individual where significant differences from a normative standard occur by using a hot-to-cold display, such as may be achieved using the Advanced Normalization Tools (ANTs) program (<http://stnava.github.io/ANTs/>; see Tustison et al. 2014). Hot-to-warm colors (reds to orange) signify regions larger in the subject than found in the normative comparison, where cold colors (shades of blue) signify reduced volume.

Applying the cortical deformation mapping as shown in Fig. 18, this image, within a basic cortical surface rendered display captures the simultaneous reductions in frontal and

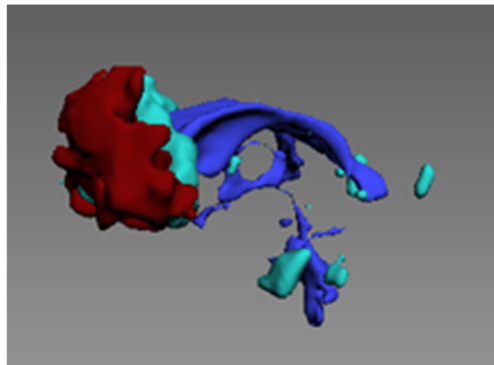


**Fig. 19** Left frontal oblique view of the large area of focal encephalomalacia (red) of the case shown in Fig. 18, which is the same lesion depicted in the upper left. The ventricular system, shown in blue, is merely presented for reference and as an anatomical landmark. By applying the automated WM analysis method outlined by Schmidt et al. (2012b) to the FLAIR sequence, regions of WM hyperintense signal may be identified (shown in aquamarine), isolated and presented in 3-D. In this manner either specific signal abnormalities are identified or summed to generate an overall lesion burden volume indicating WM structural damage. The “total” lesion volume would be the combined regions colorized in red and aquamarine. However, since there are atrophic changes, as shown in Fig. 18, actual brain pathology is greater than just the visible focal lesions

temporal polar areas (regions depicted in blue) and the increase in ventricular size (secondary to hydrocephalus ex-vacuo depicted in red).

So what is the damage? It is likely best reflected in a combination of all of the above MR sequences and image analysis techniques.

This TBI example demonstrates the complexity of structural neuroimaging analyses to document pathology. Most disorders will have a heterogeneity component. For example, while a large focal vascular accident may appear to be just that, focal damage from a large stroke, the actual extent of the penumbra may involve subtle distal pathologies extending out far from the core areas of damage (Maillard et al. 2011). Furthermore underlying reasons for the stroke likely means other factors are also involved (i.e., non-specific vascular disease, hypertension, metabolic disorder, etc.) suggesting associated pathologies are likely present as well, some not necessarily macroscopically identifiable using neuroimaging methods. Accordingly, just like the TBI case presented in Figs. 16, 17, 18 and 19 demonstrates, a single metric of brain anatomy, reflecting either integrity or pathology, is likely insufficient to capture the full complexity of the neuropathology that may be present in any neurological or neuropsychiatric disorder.

Because of the potential heterogeneity in the distribution of lesions and how measured in structural imaging, neuropsychology has likely made major methodological errors in underestimating the size, extent and distribution of neuropathology. This is certainly true in TBI studies where the assumption has been that TBI would produce some kind of uniform injury or damage, but as shown by the case presented in this review,

the definition and size of the abnormality depends on the MR sequence used and the image analysis tools applied. Studies that apply multimodal and multivariate analyses to neuroimaging metrics better approximate the complexities of brain-behavior relations linking neurobehavioral findings to structural imaging as shown in the study by Cook et al. (2014), including applications of machine learning (Hellyer et al. 2013).

Finally, Bilder (2011) provides guidelines for the future role of neuroimaging, including structural neuroimaging metrics, in neuropsychology. It is not just the neuroimaging finding but the integration and relation with neuroinformatics, genetics and neuropsychological assessment tools that will reveal brain-behavioral correlates. Complex datasets comprised of neuroimaging and neuropsychological variables may be explored with computational learning tools and other techniques that likely will yield better understanding of brain-behavior relations (Atluri et al. 2013; Lichtman et al. 2014; Varoquaux and Thirion 2014). Neuropsychology has now entered the era of the human connectome project, and the challenges that go along with large datasets (Lichtman et al. 2014), results from which will also inform the field on the relation between brain structure and function (Barch et al. 2013).

### Contemporary Examples of Structural Neuroimaging Findings in Neuropsychology

By midyear 2015, when this review was written, the number of studies using voxel-based image analysis methods number in the thousands with FreeSurfer based studies now over 600. The majority of these studies examine some cognitive or neurobehavioral variable far beyond the scope of this review to summarize. Nevertheless, in the arena of cognitive assessment neuropsychological test findings may now be explored in relation to neuroimaging defined anatomical and pathological correlates for *all* conditions and disorders. Traditionally neuropsychological tasks have been divided into the customary areas of motor, sensory-perceptual, language, visuospatial, speed of processing/executive functioning and emotional control when compared to neuroimaging findings (see Zahodne et al. 2015). Using these different neuropsychological domains a brief overview of contemporary findings mainly using the T1-weighted FreeSurfer technique is provided below.

**Motor** In the traditional neuropsychological test battery motor function is assessed with tasks that involve finger tapping, strength of grip along with measures of manual dexterity (Lezak et al. 2012). Using FreeSurfer derived volumes of the motor cortex (pre-central gyrus), Kwan et al. (2012) have shown its relation to finger tapping in both healthy controls as well as those with motor neuron disorders. In an autism spectrum disorder sample, Duffield et al. (2013) demonstrated that finger tapping speed was negatively correlated with FreeSurfer derived motor cortex volume. Koppelmans et al.

(2015) used FreeSurfer to explore motor control relations of cerebellar gray and white matter in healthy adults showing mostly positive correlates of regional cerebellar white and gray matter volumes with motor performance. Because of the extensiveness and complexity of cerebellar folia, the cerebellum has been a brain region that constituted a major challenge for manual image analysis, which is overcome by contemporary automated image analysis techniques. Future studies of the motor system using FreeSurfer will likely reveal important new information about how motor impairments on traditional neuropsychological measures relate to underlying brain pathology.

**Sensory** In disorders associated with altered sensory function, most neuroimaging work has focused on functional rather than structural imaging. To date neuropsychological outcome studies have mostly used basic VBM techniques in relation to cortical areas of sensory function (Nocentini et al. 2014; Sastre-Garriga et al. 2009). Gabilondo et al. (2014) related FreeSurfer determined visual cortex volume to optic nerve atrophy and impaired visual processing in patients with multiple sclerosis. Tate et al. (2014) used FreeSurfer to explore cortical thickness in blast injured service members and found thinning in the region of auditory cortex to be related to audiological deficits and tinnitus, presumed to reflect the cortical response to altered auditory input.

**Language** Much of FreeSurfer use in language disorder has centered on changes associated with dementia, in particular primary progressive aphasia ((Leyton et al. 2015; Rogalski et al. 2014). Since the structural damage from stroke may be best characterized by T2-weighted FLAIR and SWI techniques, the T1-weighted basis for FreeSurfer likely underestimates lesion burden. Additionally, as structural damage increases the anatomical distortion from large vascular lesions creates problems for automated segmentation and classification. Various automated methods for lesion quantification are being developed for the stroke patient to overcome the above limitations (Shi et al. 2013). Since correction procedures are being developed for a variety of structural image analysis methods (Toga 2015), undoubtedly such studies will be forthcoming.

**Memory** The most frequently studied neuropsychological variable in association with quantitative neuroimaging is memory. Using FreeSurfer Meiberth et al (2015) found reduced cortical thickness to be associated with subjective memory impairment and Jak et al. (2015) found correlates of reduced FreeSurfer derived hippocampal volumetry and neuropsychological performance in individuals with mild cognitive impairment. Also, the latest versions of FreeSurfer includes a hippocampal subfield segmentation package. However, Wisse, Biessels and Geerlings (Wisse et al. 2014) raise

cautionary comments about the subfield segmentation routine in studies not done with high resolution 3 T imaging.

**Executive Function (EF)** Gautam, Anstey, Wen, Sachdev, and Cherbuin (Gautam et al. 2015) used the Symbol-Digit Modalities Test (SDMT) along with the Trail Making Test (Lezak et al. 2012 for test explanation and details) as EF measures and digit span (backwards) as an index of working memory in an examination of cortical volume, thickness and gyration in a large sample of healthy middle-aged adults. These investigators demonstrated that greater cortical gyration was related both to bigger brain volume and better cognitive function, but not to greater cortical thickness. Frontal gyration was positively related to performance in working memory and mental flexibility tasks. In MS corpus callosum volumetry assessed by FreeSurfer has been shown to positively relate to SDMT performance (Granberg et al. 2014). The Krueger et al. (2011) study differentiating orbitofrontal from dorsolateral associated with EF and emotional control has already been discussed.

**Visuospatial** Most studies that have examined brain structure using FreeSurfer in relation to visuospatial abilities have focused on age-related decline and degenerative diseases like Alzheimer's (Garcia-Diaz et al. 2014; Lehmann et al. 2011); however, in an adolescent sample Squeglia et al. (2013) showed that FreeSurfer derived cortical thickness measures related to visuospatial functioning, where thinner parietal cortices were found in those with better visuospatial abilities.

**Emotional** Maller et al. (2014) used FreeSurfer to explore volumetric changes associated with mild TBI and how those changes related to those who developed major depression. Severity of depression post mild TBI was correlated with reduced volume in the anterior cingulate, temporal lobe and insula. Jones et al. (2015) found larger volume of the amygdala as derived from FreeSurfer to be associated with increased levels of anxiety in children with epilepsy. Reduced OFC was also related to higher levels of reported anxiety which would be consistent with poorer emotional control as reported in the Krueger et al. (2011) study previously discussed.

## Summary

Numerous well established neuroimaging methods for analyzing structural imaging findings from MRI have been reviewed. Excellent techniques for identifying size, thickness, surface area, shape and contour are available for the field of neuropsychology to explore anatomical and pathological relations. This review focused on just the structural side of neuroimaging analyses but contemporary neuroimaging yields numerous other methods that can be integrated with structural

imaging for a multimodal MR approach to understanding brain-behavior relations (Goh et al. 2014, 2015; Hasan et al. 2012; Sui et al. 2015). The next few decades of basic and clinical research will likely provide a rich array of quantitative methods for image analysis for all aspects of neuropsychology.

**Acknowledgments** Aspects of the research reviewed in this article were supported by the U.S. Army Medical Research and Material Command under Award No. W81XWH-13-2-0095 (Chronic Effects of Neurotrauma Consortium). The views and opinions expressed in this article are those of the author and do not necessarily reflect the position or the policy of the Government, and no official endorsement should be inferred. Dr. Bigler co-directs the Neuropsychological Assessment and Research Laboratory at Brigham Young University which provides forensic consultation.

## References

- Akert, J. M., & Warren, K. (1964). *The frontal granular cortex and behavior*. New York: McGraw-Hill.
- Arndt, S., Cohen, G., Alliger, R. J., Swayze, V. W., 2nd, & Andreasen, N. C. (1991). Problems with ratio and proportion measures of imaged cerebral structures. [Research Support, Non-U.S. Gov't Research Support, U.S. Gov't, P.H.S.]. *Psychiatry Research*, 40(1), 79–89.
- Ashburner, J., & Friston, K. J. (2000). Voxel-based morphometry—the methods. *NeuroImage*, 11(6 Pt 1), 805–821. doi:10.1006/nimg.2000.0582.
- Atluri, G., Padmanabhan, K., Fang, G., Steinbach, M., Petrella, J. R., Lim, K., & Kumar, V. (2013). Complex biomarker discovery in neuroimaging data: finding a needle in a haystack. [Review]. *NeuroImage Clinical*, 3, 123–131. doi:10.1016/j.nicl.2013.07.004.
- Barch, D. M., Burgess, G. C., Harms, M. P., Petersen, S. E., Schlaggar, B. L., Corbetta, M., & Van Essen, D. C. (2013). Function in the human connectome: task-fMRI and individual differences in behavior. *NeuroImage*, 80, 169–189. doi:10.1016/j.neuroimage.2013.05.033.
- Barton, R. A. (2006). Olfactory evolution and behavioral ecology in primates. *American Journal of Primatology*, 68(6), 545–558. doi:10.1002/ajp.20251.
- Bates, E., Wilson, S. M., Saygin, A. P., Dick, F., Sereno, M. I., Knight, R. T., & Dronkers, N. F. (2003). Voxel-based lesion-symptom mapping. [Comparative Study Research Support, U.S. Gov't, Non-P.H.S. Research Support, U.S. Gov't, P.H.S.]. *Nature Neuroscience*, 6(5), 448–450. doi:10.1038/nn1050.
- Bergeson, A. G., Lundin, R., Parkinson, R. B., Tate, D. F., Victoroff, J., Hopkins, R. O., & Bigler, E. D. (2004). Clinical rating of cortical atrophy and cognitive correlates following traumatic brain injury. *Clinical Neuropsychology*, 18(4), 509–520. doi:10.1080/1385404049052414.
- Bigler, E. D. (1996a). *Neuroimaging I. Basic science*. New York: Plenum Press.
- Bigler, E. D. (1996b). *Neuroimaging II. Clinical applications*. New York: Plenum Press.
- Bigler, E. D., Hubler, D. W., Cullum, C. M., & Turkheimer, E. (1985). Intellectual and memory impairment in dementia. Computerized axial tomography volume correlations. *The Journal of Nervous and Mental Disease*, 173(6), 347–352.
- Bigler, E. D., Yeo, R. A., & Turkheimer, E. (1989). *Neuropsychological function and brain imaging*. New York: Plenum Press.
- Bigler, E. D., Blatter, D. D., Anderson, C. V., Johnson, S. C., Gale, S. D., Hopkins, R. O., & Burnett, B. (1997). Hippocampal volume in normal aging and traumatic brain injury. *AJNR - American Journal of Neuroradiology*, 18(1), 11–23.
- Bigler, E. D., Abildskov, T. J., Wilde, E. A., McCauley, S. R., Li, X., Merkley, T. L., & Levin, H. S. (2010). Diffuse damage in pediatric traumatic brain injury: a comparison of automated versus operator-controlled quantification methods. *NeuroImage*, 50(3), 1017–1026. doi:10.1016/j.neuroimage.2010.01.003.
- Bigler, E. D., Abildskov, T. J., Petrie, J., Farrer, T. J., Dennis, M., Simic, N., & Owen Yeates, K. (2013). Heterogeneity of brain lesions in pediatric traumatic brain injury. *Neuropsychology*, 27(4), 438–451. doi:10.1037/a0032837.
- Bilder, R. M. (2011). Neuropsychology 3.0: evidence-based science and practice. [Historical Article Research Support, N.I.H., ExtramuralResearch Support, Non-U.S. Gov't Review]. *Journal of International Neuropsychological Society*, 17(1), 7–13. doi:10.1017/S1355617710001396.
- Bitar, R., Leung, G., Perng, R., Tadros, S., Moody, A. R., Sarrazin, J., & Roberts, T. P. (2006). MR pulse sequences: what every radiologist wants to know but is afraid to ask. *Radiographics*, 26(2), 513–537. doi:10.1148/rq.262055063.
- Blatter, D. D., Bigler, E. D., Gale, S. D., Johnson, S. C., Anderson, C. V., Burnett, B. M., & Horn, S. D. (1995). Quantitative volumetric analysis of brain MR: normative database spanning 5 decades of life. *AJNR - American Journal of Neuroradiology*, 16(2), 241–251.
- Booker, H. E., Matthews, C. G., & Whitehurst, W. R. (1969). Pneumoencephalographic planimetry in neurological disease. *Journal of Neurology, Neurosurgery, and Psychiatry*, 32(3), 241–248.
- Botez, M. I., Fontaine, F., Botez, T., & Bachevalier, J. (1977). Folate-responsive neurological and mental disorders: report of 16 cases. Neuropsychological correlates of computerized transaxial tomography and radionuclide cisternography in folic acid deficiencies. *European Neurology*, 16(1-6), 230–246.
- Brewer, J. B. (2009). Fully-automated volumetric MRI with normative ranges: translation to clinical practice. *Behavioural Neurology*, 21(1), 21–28. doi:10.3233/BEN-2009-0226.
- Buschhuter, D., Smitka, M., Puschmann, S., Gerber, J. C., Witt, M., Abolmaali, N. D., & Hummel, T. (2008). Correlation between olfactory bulb volume and olfactory function. *NeuroImage*, 42(2), 498–502. doi:10.1016/j.neuroimage.2008.05.004.
- Campana, S., Caltagirone, C., & Marangolo, P. (2015). Combining voxel-based lesion-symptom mapping (VLSM) with A-tDCS language treatment: predicting outcome of recovery in nonfluent chronic aphasia. *Brain Stimulation*. doi:10.1016/j.brs.2015.01.413.
- Catani, M., Dell'acqua, F., Bizzi, A., Forkel, S. J., Williams, S. C., Simmons, A., & Thiebaut de Schotten, M. (2012). Beyond cortical localization in clinico-anatomical correlation. *Cortex*, 48(10), 1262–1287. doi:10.1016/j.cortex.2012.07.001.
- Chalavi, S., Simmons, A., Dijkstra, H., Barker, G. J., & Reinders, A. A. (2012). Quantitative and qualitative assessment of structural magnetic resonance imaging data in a two-center study. [Evaluation Studies Multicenter Study Research Support, Non-U.S. Gov't]. *BMC Medical Imaging*, 12, 27. doi:10.1186/1471-2342-12-27.
- Chau, W., & McIntosh, A. R. (2005). The Talairach coordinate of a point in the MNI space: how to interpret it. *NeuroImage*, 25(2), 408–416. doi:10.1016/j.neuroimage.2004.12.007.
- Christensen, A.-L., Goldberg, E., & Bougakov, D. (2009). *Luria's legacy in the 21st century*. New York: Oxford University Press.
- Cipolotti, L., & Warrington, E. K. (1995). Neuropsychological assessment. [Review]. *Journal of Neurology, Neurosurgery, and Psychiatry*, 58(6), 655–664.
- Clerx, L., Gronenchild, E. H., Echavarri, C., Verhey, F., Aalten, P., & Jacobs, H. I. (2015). Can FreeSurfer compete with manual volumetric measurements in Alzheimer's disease? *Current Alzheimer Research*, 12(4), 358–367.

- Collins, A. F. (2006). An intimate connection: Oliver Zangwill and the emergence of neuropsychology in Britain. [Biography Historical Article Research Support, Non-U.S. Gov't]. *History of Psychology*, 9(2), 89–112.
- Cook, P. A., McMillan, C. T., Avants, B. B., Peelle, J. E., Gee, J. C., & Grossman, M. (2014). Relating brain anatomy and cognitive ability using a multivariate multimodal framework. *NeuroImage*, 99, 477–486. doi:10.1016/j.neuroimage.2014.05.008.
- Cox, S. R., Ferguson, K. J., Royle, N. A., Shenkin, S. D., MacPherson, S. E., MacLullich, A. M., & Wardlaw, J. M. (2014). A systematic review of brain frontal lobe parcellation techniques in magnetic resonance imaging. *Brain Structure and Function*, 219(1), 1–22. doi:10.1007/s00429-013-0527-5.
- Cullum, C. M., & Bigler, E. D. (1986). Ventricle size, cortical atrophy and the relationship with neuropsychological status in closed head injury: a quantitative analysis. *Journal of Clinical and Experimental Neuropsychology*, 8(4), 437–452. doi:10.1080/01688638608401333.
- Dale, A. M., Fischl, B., & Sereno, M. I. (1999). Cortical surface-based analysis I. Segmentation and surface reconstruction. *NeuroImage*, 9(2), 179–194. doi:10.1006/nimg.1998.0395.
- Davies, R. R., Seahill, V. L., Graham, A., Williams, G. B., Graham, K. S., & Hodges, J. R. (2009). Development of an MRI rating scale for multiple brain regions: comparison with volumetrics and with voxel-based morphometry. *Neuroradiology*, 51(8), 491–503. doi:10.1007/s00234-009-0521-z.
- DeCarli, C., Frisoni, G. B., Clark, C. M., Harvey, D., Grundman, M., Petersen, R. C., & Alzheimer's Disease Cooperative Study, G. (2007). Qualitative estimates of medial temporal atrophy as a predictor of progression from mild cognitive impairment to dementia. *Archives of Neurology*, 64(1), 108–115. doi:10.1001/archneur.64.1.108.
- Delano-Wood, L., Bondi, M. W., Sacco, J., Abeles, N., Jak, A. J., Libon, D. J., & Bozoki, A. (2009). Heterogeneity in mild cognitive impairment: differences in neuropsychological profile and associated white matter lesion pathology. *Journal of International Neuropsychological Society*, 15(6), 906–914. doi:10.1017/S1355617709990257.
- Desikan, R. S., Segonne, F., Fischl, B., Quinn, B. T., Dickerson, B. C., Blacker, D., & Killiany, R. J. (2006). An automated labeling system for subdividing the human cerebral cortex on MRI scans into gyral based regions of interest. [Research Support, N.I.H., Extramural Research Support, Non-U.S. Gov't]. *NeuroImage*, 31(3), 968–980. doi:10.1016/j.neuroimage.2006.01.021.
- Destrieux, C., Fischl, B., Dale, A., & Halgren, E. (2010). Automatic parcellation of human cortical gyri and sulci using standard anatomical nomenclature. [Research Support, N.I.H., Extramural]. *NeuroImage*, 53(1), 1–15. doi:10.1016/j.neuroimage.2010.06.010.
- Diaz-de-Grenu, L. Z., Acosta-Cabronero, J., Chong, Y. F., Pereira, J. M., Sajjadi, S. A., Williams, G. B., & Nestor, P. J. (2014). A brief history of voxel-based grey matter analysis in Alzheimer's disease. [Research Support, Non-U.S. Gov't]. *Journal of Alzheimer's Disease JAD*, 38(3), 647–659. doi:10.3233/JAD-130362.
- Dolinskas, C. A., Zimmerman, R. A., Bilaniuk, L. T., & Uzzell, B. P. (1978). Correlation of long-term follow-up neurologic, psychologic, and cranial computed tomographic evaluations of head trauma patients. *Neuroradiology*, 16, 318–319.
- Drapkin, Z. A., Lindgren, K. A., Lopez, M. J., & Stabio, M. E. (2015). Development and assessment of a new 3D neuroanatomy teaching tool for MRI training. *Anatomical Sciences Education*. doi:10.1002/ase.1509.
- Duffield, T. C., Trontel, H. G., Bigler, E. D., Froehlich, A., Prigge, M. B., Travers, B., & Lainhart, J. (2013). Neuropsychological investigation of motor impairments in autism. [Research Support, N.I.H., Extramural Research Support, Non-U.S. Gov't]. *Journal of Clinical and Experimental Neuropsychology*, 35(8), 867–881. doi:10.1080/13803395.2013.827156.
- Durand-Dubief, F., Belaroussi, B., Armsbach, J. P., Dufour, M., Roggerone, S., Vukusic, S., & Cotton, F. (2012). Reliability of longitudinal brain volume loss measurements between 2 sites in patients with multiple sclerosis: comparison of 7 quantification techniques. [Comparative Study Evaluation Studies Research Support, Non-U.S. Gov't]. *AJNR - American Journal of Neuroradiology*, 33(10), 1918–1924. doi:10.3174/ajnr.A3107.
- Eling, P. (2015). Kurt Goldstein's test battery. *Cortex*, 63, 16–26. doi:10.1016/j.cortex.2014.08.002.
- Fama, R., & Sullivan, E. V. (2014). Methods of association and dissociation for establishing selective brain-behavior relations. *Handbook of Clinical Neurology*, 125, 175–181. doi:10.1016/B978-0-444-62619-6.00011-2.
- Farbota, K. D., Sodhi, A., Bendlin, B. B., McLaren, D. G., Xu, G., Rowley, H. A., & Johnson, S. C. (2012). Longitudinal volumetric changes following traumatic brain injury: a tensor-based morphometry study. *Journal of International Neuropsychological Society*, 18(6), 1006–1018. doi:10.1017/S1355617712000835.
- Fischl, B. (2012). FreeSurfer. [Historical Article Research Support, N.I.H., Extramural Research Support, Non-U.S. Gov't Review]. *NeuroImage*, 62(2), 774–781. doi:10.1016/j.neuroimage.2012.01.021.
- Fombonne, E., Roge, B., Claverie, J., Courty, S., & Fremolle, J. (1999). Microcephaly and macrocephaly in autism. *Journal of Autism and Developmental Disorders*, 29(2), 113–119.
- Frisoni, G. B., Scheltens, P., Galluzzi, S., Nobili, F. M., Fox, N. C., Robert, P. H., & Salmon, E. (2003). Neuroimaging tools to rate regional atrophy, subcortical cerebrovascular disease, and regional cerebral blood flow and metabolism: consensus paper of the EADC. *Journal of Neurology, Neurosurgery, and Psychiatry*, 74(10), 1371–1381.
- Gabilondo, I., Martinez-Lapiscina, E. H., Martinez-Heras, E., Fraga-Pumar, E., Llufrui, S., Ortiz, S., & Villoslada, P. (2014). Trans-synaptic axonal degeneration in the visual pathway in multiple sclerosis. [Research Support, Non-U.S. Gov't]. *Annals of Neurology*, 75(1), 98–107. doi:10.1002/ana.24030.
- Garcia-Diaz, A. I., Segura, B., Baggio, H. C., Marti, M. J., Valldeoriola, F., Compta, Y., & Junque, C. (2014). Structural MRI correlates of the MMSE and pentagon copying test in Parkinson's disease. [Research Support, Non-U.S. Gov't]. *Parkinsonism & Related Disorders*, 20(12), 1405–1410. doi:10.1016/j.parkreldis.2014.10.014.
- Gautam, P., Anstey, K. J., Wen, W., Sachdev, P. S., & Cherbuin, N. (2015). Cortical gyration and its relationships with cortical volume, cortical thickness, and cognitive performance in healthy mid-life adults. [Research Support, Non-U.S. Gov't]. *Behavioural Brain Research*, 287, 331–339. doi:10.1016/j.bbr.2015.03.018.
- George, A. E., de Leon, M. J., Rosenbloom, S., Ferris, S. H., Gentes, C., Emmerich, M., & Kricheff, I. I. (1983). Ventricular volume and cognitive deficit: a computed tomographic study. [Research Support, U.S. Gov't, P.H.S.]. *Radiology*, 149(2), 493–498. doi:10.1148/radiology.149.2.6622694.
- Geschwind, N. (1975). The borderland of neurology and psychiatry: Some common misconceptions. In D. Blumer & D. F. Benson (Eds.), *Psychiatric aspects of neurologic disease* (Vol. 1). New York: Grune & Stratton.
- Glascher, J., Tranel, D., Paul, L. K., Rudrauf, D., Rorden, C., Hornaday, A., & Adolphs, R. (2009). Lesion mapping of cognitive abilities linked to intelligence. [Research Support, N.I.H., Extramural Research Support, Non-U.S. Gov't]. *Neuron*, 61(5), 681–691. doi:10.1016/j.neuron.2009.01.026.
- Glascher, J., Adolphs, R., Damasio, H., Bechara, A., Rudrauf, D., Calamia, M., & Tranel, D. (2012). Lesion mapping of cognitive control and value-based decision making in the prefrontal cortex.

- [Research Support, N.I.H., Extramural Research Support, Non-U.S. Gov't]. *Proceedings of the National Academy of Sciences of the United States of America*, 109(36), 14681–14686. doi:[10.1073/pnas.1206608109](https://doi.org/10.1073/pnas.1206608109).
- Glatz, A., Bastin, M. E., Kiker, A. J., Deary, I. J., Wardlaw, J. M., & Valdes Hernandez, M. C. (2015). Automated segmentation of multifocal basal ganglia T2\*-weighted MRI hypointensities. *NeuroImage*, 105, 332–346. doi:[10.1016/j.neuroimage.2014.10.001](https://doi.org/10.1016/j.neuroimage.2014.10.001).
- Glozman, J. M. (2007). A.R. Luria and the history of Russian neuropsychology. [Biography Historical Article Portraits]. *Journal of the History of the Neurosciences*, 16(1-2), 168–180. doi:[10.1080/09647040600550368](https://doi.org/10.1080/09647040600550368).
- Goh, S. Y., Irimia, A., Torgerson, C. M., & Horn, J. D. (2014). Neuroinformatics challenges to the structural, connectomic, functional and electrophysiological multimodal imaging of human traumatic brain injury. [Review]. *Frontiers in Neuroinformatics*, 8, 19. doi:[10.3389/fninf.2014.00019](https://doi.org/10.3389/fninf.2014.00019).
- Goh, S. Y., Irimia, A., Torgerson, C. M., Tubi, M. A., Real, C. R., Hanley, D. F., & Van Horn, J. D. (2015). Longitudinal quantification and visualization of intracerebral haemorrhage using multimodal magnetic resonance and diffusion tensor imaging. [Research Support, N.I.H., Extramural]. *Brain Injury*, 29(4), 438–445. doi:[10.3109/02699052.2014.989907](https://doi.org/10.3109/02699052.2014.989907).
- Gonzalez, C. F., Lantieri, R. L., & Nathan, R. J. (1978). The CT scan appearance of the brain in the normal elderly population: a correlative study. *Neuroradiology*, 16, 120–122.
- Good, C. D., Ashburner, J., & Frackowiak, R. S. (2001). Computational neuroanatomy: new perspectives for neuroradiology. [Review]. *Revue Neurologique*, 157(8-9 Pt 1), 797–806.
- Good, C. D., Scahill, R. I., Fox, N. C., Ashburner, J., Friston, K. J., Chan, D., & Frackowiak, R. S. (2002). Automatic differentiation of anatomical patterns in the human brain: validation with studies of degenerative dementias. [Clinical Trial Research Support, Non-U.S. Gov't]. *NeuroImage*, 17(1), 29–46.
- Grafman, J., Salazar, A., Weingartner, H., Vance, S., & Amin, D. (1986). The relationship of brain-tissue loss volume and lesion location to cognitive deficit. [Research Support, U.S. Gov't, Non-P.H.S.]. *Journal of Neuroscience*, 6(2), 301–307.
- Granberg, T., Martola, J., Bergendal, G., Shams, S., Damangir, S., Aspelin, P., & Kristoffersen-Wiberg, M. (2014). Corpus callosum atrophy is strongly associated with cognitive impairment in multiple sclerosis: results of a 17-year longitudinal study. *Multiple Sclerosis*. doi:[10.1177/1352458514560928](https://doi.org/10.1177/1352458514560928).
- Green, R. E., Colella, B., Maller, J. J., Bayley, M., Glazer, J., & Mikulis, D. J. (2014). Scale and pattern of atrophy in the chronic stages of moderate-severe TBI. *Frontiers in Human Neuroscience*, 8, 67. doi:[10.3389/fnhum.2014.00067](https://doi.org/10.3389/fnhum.2014.00067).
- Gronenschild, E. H., Habets, P., Jacobs, H. I., Mengelers, R., Rozendaal, N., van Os, J., & Marcelis, M. (2012). The effects of FreeSurfer version, workstation type, and Macintosh operating system version on anatomical volume and cortical thickness measurements. [Research Support, Non-U.S. Gov't]. *PLoS ONE*, 7(6), e38234. doi:[10.1371/journal.pone.0038234](https://doi.org/10.1371/journal.pone.0038234).
- Haas, L. F. (2001). Phineas gage and the science of brain localisation. [Biography Historical Article Portraits]. *Journal of Neurology, Neurosurgery, and Psychiatry*, 71(6), 761.
- Haehner, A., Rodewald, A., Gerber, J. C., & Hummel, T. (2008). Correlation of olfactory function with changes in the volume of the human olfactory bulb. *Archives of Otolaryngology - Head and Neck Surgery*, 134(6), 621–624. doi:[10.1001/archotol.134.6.621](https://doi.org/10.1001/archotol.134.6.621).
- Hanggi, J., Fovenyi, L., Liem, F., Meyer, M., & Jancke, L. (2014). The hypothesis of neuronal interconnectivity as a function of brain size-a general organization principle of the human connectome. *Frontiers in Human Neuroscience*, 8, 915. doi:[10.3389/fnhum.2014.00915](https://doi.org/10.3389/fnhum.2014.00915).
- Hasan, K. M., Walimuni, I. S., Abid, H., Datta, S., Wolinsky, J. S., & Narayana, P. A. (2012). Human brain atlas-based multimodal MRI analysis of volumetry, diffusometry, relaxometry and lesion distribution in multiple sclerosis patients and healthy adult controls: implications for understanding the pathogenesis of multiple sclerosis and consolidation of quantitative MRI results in MS. [Comparative Study Research Support, N.I.H., Extramural Research Support, Non-U.S. Gov't]. *Journal of Neurological Sciences*, 313(1-2), 99–109. doi:[10.1016/j.jns.2011.09.015](https://doi.org/10.1016/j.jns.2011.09.015).
- Hashemi, R. H., & Bradley, W. G. (2010). *MRI: The basics*. Philadelphia: Lippincott Williams & Wilkins.
- Hecaen, H., & Albert, M. L. (1978). *Human neuropsychology*. New York: Wiley.
- Heindel, W. C., Jernigan, T. L., Archibald, S. L., Achim, C. L., Masliah, E., & Wiley, C. A. (1994). The relationship of quantitative brain magnetic resonance imaging measures to neuropathologic indexes of human immunodeficiency virus infection. [Research Support, U.S. Gov't, Non-P.H.S. Research Support, U.S. Gov't, P.H.S.]. *Archives of Neurology*, 51(11), 1129–1135.
- Hellyer, P. J., Leech, R., Ham, T. E., Bonnelle, V., & Sharp, D. J. (2013). Individual prediction of white matter injury following traumatic brain injury. [Research Support, Non-U.S. Gov't]. *Annals of Neurology*, 73(4), 489–499. doi:[10.1002/ana.23824](https://doi.org/10.1002/ana.23824).
- Hounsfield, G. N. (1973). Computerized transverse axial scanning (tomography). 1. Description of system. *British Journal of Radiology*, 46(552), 1016–1022. doi:[10.1259/0007-1285-46-552-1016](https://doi.org/10.1259/0007-1285-46-552-1016).
- Hummel, T., Smitka, M., Puschmann, S., Gerber, J. C., Schaaf, B., & Buschhuter, D. (2011). Correlation between olfactory bulb volume and olfactory function in children and adolescents. *Experimental Brain Research*, 214(2), 285–291. doi:[10.1007/s00221-011-2832-7](https://doi.org/10.1007/s00221-011-2832-7).
- Iscan, Z., Jin, T. B., Kendrick, A., Szeglin, B., Lu, H., Trivedi, M., & DeLorenzo, C. (2015). Test-retest reliability of freesurfer measurements within and between sites: effects of visual approval process. *Human Brain Mapping*. doi:[10.1002/hbm.22856](https://doi.org/10.1002/hbm.22856).
- Jak, A. J., Panizzon, M. S., Spoon, K. M., Fennema-Notestine, C., Franz, C. E., Thompson, W. K., & Kremen, W. S. (2015). Hippocampal atrophy varies by neuropsychologically defined MCI among men in their 50s. [Research Support, N.I.H., Extramural Research Support, Non-U.S. Gov't Research Support, U.S. Gov't, Non-P.H.S.]. *The American Journal of Geriatric Psychiatry : Official Journal of the American Association for Geriatric Psychiatry*, 23(5), 456–465. doi:[10.1016/j.jagp.2014.08.011](https://doi.org/10.1016/j.jagp.2014.08.011).
- Jernigan, T. L., Zatz, L. M., Ahumada, A. J., Jr., Pfefferbaum, A., Tinklenberg, J. R., & Moses, J. A., Jr. (1982a). CT measures of cerebrospinal fluid volume in alcoholics and normal volunteers. [Research Support, U.S. Gov't, Non-P.H.S.]. *Psychiatry Research*, 7(1), 9–17.
- Jernigan, T. L., Zatz, L. M., Moses, J. A., Jr., & Berger, P. A. (1982b). Computed tomography in schizophrenics and normal volunteers. I. Fluid volume. [Research Support, U.S. Gov't, Non-P.H.S. Research Support, U.S. Gov't, P.H.S.]. *Archives of General Psychiatry*, 39(7), 765–770.
- Jernigan, T. L., Zatz, L. M., Moses, J. A., Jr., & Cardellino, J. P. (1982c). Computed tomography in schizophrenics and normal volunteers. II. Cranial asymmetry. [Research Support, U.S. Gov't, P.H.S.]. *Archives of General Psychiatry*, 39(7), 771–773.
- Jones, J. E., Jackson, D. C., Chambers, K. L., Dabbs, K., Hsu, D. A., Stafstrom, C. E., & Hermann, B. P. (2015). Children with epilepsy and anxiety: subcortical and cortical differences. [Research Support, N.I.H., Extramural Research Support, Non-U.S. Gov't]. *Epilepsia*, 56(2), 283–290. doi:[10.1111/epi.12832](https://doi.org/10.1111/epi.12832).
- Kennedy, K. M., Erickson, K. I., Rodriguez, K. M., Voss, M. W., Colcombe, S. J., Kramer, A. F., & Raz, N. (2009). Age-related differences in regional brain volumes: a comparison of optimized voxel-based morphometry to manual volumetry. [Comparative Study Research Support, N.I.H., Extramural]. *Neurobiology of Aging*, 30(10), 1553–1562.

- Aging*, 30(10), 1657–1676. doi:10.1016/j.neurobiolaging.2007.12.020.
- Kertesz, A. (1984). *Localization in neuropsychology*. San Diego: Academic.
- Kertesz, A. (1994). *Localization and neuroimaging in neuropsychology*. San Diego: Academic.
- Kessler, D., Angstadt, M., Welsh, R. C., & Sripada, C. (2014). Modality-spanning deficits in attention-deficit/hyperactivity disorder in functional networks, gray matter, and white matter. *Journal of Neuroscience*, 34(50), 16555–16566. doi:10.1523/JNEUROSCI.3156-14.2014.
- Koppelmans, V., Hirsiger, S., Merillat, S., Jancke, L., & Seidler, R. D. (2015). Cerebellar gray and white matter volume and their relation with age and manual motor performance in healthy older adults. [Research Support, Non-U.S. Gov't]. *Human Brain Mapping*, 36(6), 2352–2363. doi:10.1002/hbm.22775.
- Krueger, C. E., Laluz, V., Rosen, H. J., Neuhaus, J. M., Miller, B. L., & Kramer, J. H. (2011). Double dissociation in the anatomy of socioemotional disinhibition and executive functioning in dementia. [Research Support, N.I.H., Extramural Research Support, Non-U.S. Gov't]. *Neuropsychology*, 25(2), 249–259. doi:10.1037/a0021681.
- Kwan, J. Y., Meoded, A., Danielian, L. E., Wu, T., & Floeter, M. K. (2012). Structural imaging differences and longitudinal changes in primary lateral sclerosis and amyotrophic lateral sclerosis. *NeuroImage Clinical*, 2, 151–160. doi:10.1016/j.nicl.2012.12.003.
- Laakso, M., Soiminin, H., Partanen, K., Hallikainen, M., Lehtovirta, M., Hanninen, T., & Riekkinen, P. J., Sr. (1995). The interuncal distance in Alzheimer disease and age-associated memory impairment. [Research Support, Non-U.S. Gov't]. *AJNR - American Journal of Neuroradiology*, 16(4), 727–734.
- Lange, N., Froimowitz, M. P., Bigler, E. D., Lainhart, J. E., & Brain Development Cooperative, G. (2010). Associations between IQ, total and regional brain volumes, and demography in a large normative sample of healthy children and adolescents. *Developmental Neuropsychology*, 35(3), 296–317. doi:10.1080/87565641003696833.
- Lehmann, M., Crutch, S. J., Ridgway, G. R., Ridha, B. H., Barnes, J., Warrington, E. K., & Fox, N. C. (2011). Cortical thickness and voxel-based morphometry in posterior cortical atrophy and typical Alzheimer's disease. [Comparative Study Research Support, Non-U.S. Gov't]. *Neurobiology of Aging*, 32(8), 1466–1476. doi:10.1016/j.neurobiolaging.2009.08.017.
- Levin, J. R. (1997). Overcoming feelings of powerlessness in “aging” researchers: a primer on statistical power in analysis of variance designs. [Review]. *Psychology and Aging*, 12(1), 84–106.
- Leyton, C. E., Hodges, J. R., McLean, C. A., Kril, J. J., Piguet, O., & Ballard, K. J. (2015). Is the logopenic-variant of primary progressive aphasia a unitary disorder? *Cortex*, 67, 122–133. doi:10.1016/j.cortex.2015.03.011.
- Lezak, M. D., Howieson, D. B., Bigler, E. D., & Tranel, D. (2012). *Neuropsychological assessment*. New York: Oxford University Press.
- Lichtman, J. W., Pfister, H., & Shavit, N. (2014). The big data challenges of connectomics. [Research Support, N.I.H., Extramural Research Support, Non-U.S. Gov't Research Support, U.S. Gov't, Non-P.H.S. Review]. *Nature Neuroscience*, 17(11), 1448–1454. doi:10.1038/nrn.3837.
- Liem, F., Merillat, S., Bezzola, L., Hirsiger, S., Philipp, M., Madhyastha, T., & Jancke, L. (2015). Reliability and statistical power analysis of cortical and subcortical FreeSurfer metrics in a large sample of healthy elderly. *NeuroImage*, 108, 95–109. doi:10.1016/j.neuroimage.2014.12.035.
- Liu, D., Johnson, H. J., Long, J. D., Magnotta, V. A., & Paulsen, J. S. (2014). The power-proportion method for intracranial volume correction in volumetric imaging analysis. *Frontiers in Neuroscience*, 8, 356. doi:10.3389/fnins.2014.00356.
- Luders, E., Narr, K. L., Thompson, P. M., & Toga, A. W. (2009). Neuroanatomical correlates of intelligence. *Intelligence*, 37(2), 156–163. doi:10.1016/j.intell.2008.07.002.
- Luria, A. R. (1962). *Higher cortical functions in man*. Moscow: Moscow University Press.
- Maillard, P., Fletcher, E., Harvey, D., Carmichael, O., Reed, B., Mungas, D., & DeCarli, C. (2011). White matter hyperintensity penumbra. [Research Support, N.I.H., Extramural]. *Stroke A Journal of Cerebral Circulation*, 42(7), 1917–1922. doi:10.1161/STROKEAHA.110.609768.
- Makris, N., Kaiser, J., Haselgrave, C., Seidman, L. J., Biederman, J., Boriel, D., & Kennedy, D. N. (2006). Human cerebral cortex: a system for the integration of volume- and surface-based representations. *NeuroImage*, 33(1), 139–153. doi:10.1016/j.neuroimage.2006.04.220.
- Maller, J. J., Thomson, R. H., Pannek, K., Bailey, N., Lewis, P. M., & Fitzgerald, P. B. (2014). Volumetrics relate to the development of depression after traumatic brain injury. [Research Support, Non-U.S. Gov't]. *Behavioural Brain Research*, 271, 147–153. doi:10.1016/j.bbr.2014.05.047.
- Mathalon, D. H., Sullivan, E. V., Rawles, J. M., & Pfefferbaum, A. (1993). Correction for head size in brain-imaging measurements. [Comparative Study Research Support, Non-U.S. Gov't Research Support, U.S. Gov't, Non-P.H.S. Research Support, U.S. Gov't, P.H.S.J.]. *Psychiatry Research*, 50(2), 121–139.
- Matthews, C. G., & Booker, H. E. (1972). Pneumoencephalographic measurements and neuropsychological test performance in human adults. *Cortex*, 8(1), 69–92.
- Meiberth, D., Scheef, L., Wolfsgruber, S., Boecker, H., Block, W., Traber, F., & Jessen, F. (2015). Cortical thinning in individuals with subjective memory impairment. [Research Support, Non-U.S. Gov't]. *Journal of Alzheimer's Disease JAD*, 45(1), 139–146. doi:10.3233/JAD-142322.
- Millis, S. (2003). Statistical practices: the seven deadly sins. *Child Neuropsychology A Journal on Normal and Abnormal Development in Childhood and Adolescence*, 9(3), 221–233. doi:10.1076/chin.9.3.221.16455.
- Mirzaa, G. M., & Poduri, A. (2014). Megalencephaly and hemimegalencephaly: breakthroughs in molecular etiology. *American Journal of Medical Genetics Part C: Seminars in Medical Genetics*, 166C(2), 156–172. doi:10.1002/ajmg.c.31401.
- Naeser, M. A., & Hayward, R. W. (1978). Lesion localization in aphasia with cranial computed tomography and the Boston diagnostic aphasia exam. *Neurology*, 28(6), 545–551.
- Naeser, M. A., Hayward, R. W., Laughlin, S. A., Becker, J. M., Jernigan, T. L., & Zatz, L. M. (1981). Quantitative CT scan studies in aphasia II. Comparison of the right and left hemispheres. [Comparative Study Research Support, U.S. Gov't, P.H.S.J.]. *Brain and Language*, 12(1), 165–189.
- Nakamura, K., Guizard, N., Fonov, V. S., Narayanan, S., Collins, D. L., & Arnold, D. L. (2014). Jacobian integration method increases the statistical power to measure gray matter atrophy in multiple sclerosis. [Randomized Controlled Trial Research Support, Non-U.S. Gov't]. *NeuroImage Clinical*, 4, 10–17. doi:10.1016/j.nicl.2013.10.015.
- Ng, K., Mikulis, D. J., Glazer, J., Kabani, N., Till, C., Greenberg, G., & Green, R. E. (2008). Magnetic resonance imaging evidence of progression of subacute brain atrophy in moderate to severe traumatic brain injury. *Archives of Physical Medicine and Rehabilitation*, 89(12 Suppl), S35–S44. doi:10.1016/j.apmr.2008.07.006.
- Nocentini, U., Bozzali, M., Spano, B., Cercignani, M., Serra, L., Basile, B., & De Luca, J. (2014). Exploration of the relationships between regional grey matter atrophy and cognition in multiple sclerosis. [Research Support, Non-U.S. Gov't]. *Brain Imaging and Behavior*, 8(3), 378–386. doi:10.1007/s11682-012-9170-7.

- Ochs, A. L., Ross, D. E., Zannoni, M. D., Abildskov, T. J., & Bigler, E. D. (2015). Comparison of automated brain volume measures obtained with NeuroQuant(R) and FreeSurfer. *Journal of Neuroimaging Official Journal of the American Society of Neuroimaging*. doi:10.1111/jon.12229.
- Olesen, P. J., Guo, X., Gustafson, D., Borjesson-Hanson, A., Sacuiu, S., Eckstrom, C., & Skoog, I. (2011). A population-based study on the influence of brain atrophy on 20-year survival after age 85. *Neurology*, 76(10), 879–886. doi:10.1212/WNL.0b013e31820f2e26.
- Pfefferbaum, A., Rosenbloom, M., Crusan, K., & Jernigan, T. L. (1988). Brain CT changes in alcoholics: effects of age and alcohol consumption. [Research Support, U.S. Gov't, Non-P.H.S. Research Support, U.S. Gov't, P.H.S.]. *Alcoholism: Clinical and Experimental Research*, 12(1), 81–87.
- Pfefferbaum, A., Sullivan, E. V., Jernigan, T. L., Zipursky, R. B., Rosenbloom, M. J., Yesavage, J. A., & Tinklenberg, J. R. (1990). A quantitative analysis of CT and cognitive measures in normal aging and Alzheimer's disease. [Research Support, U.S. Gov't, Non-P.H.S. Research Support, U.S. Gov't, P.H.S.]. *Psychiatry Research*, 35(2), 115–136.
- Pfefferbaum, A., Sullivan, E. V., Adalsteinsson, E., Garrick, T., & Harper, C. (2004). Postmortem MR imaging of formalin-fixed human brain. [Research Support, U.S. Gov't, P.H.S.]. *NeuroImage*, 21(4), 1585–1595. doi:10.1016/j.neuroimage.2003.11.024.
- Plewes, D. B., & Kucharczyk, W. (2012). Physics of MRI: a primer. *Journal of Magnetic Resonance Imaging*, 35(5), 1038–1054. doi:10.1002/jmri.23642.
- Prins, N. D., & Scheltens, P. (2015). White matter hyperintensities, cognitive impairment and dementia: an update. [Review]. *Nature reviews. Neurology*, 11(3), 157–165. doi:10.1038/nrneurol.2015.10.
- Ragan, D. K., Cerqua, J., Nash, T., McKinstry, R. C., Shimony, J. S., Jones, B. V., Limbrick, D. D., Jr. (2015). The accuracy of linear indices of ventricular volume in pediatric hydrocephalus: technical note. *Journal of Neurosurgery: Pediatrics*, 1–5. doi: 10.3171/2014.10.PEDS14209.
- Raz, N., Raz, S., Yeo, R. A., Turkheimer, E., Bigler, E. D., & Cullum, C. M. (1987). Relationship between cognitive and morphological asymmetry in dementia of the Alzheimer type: a CT scan study. *The International Journal of Neuroscience*, 35(3-4), 225–232.
- Rimol, L. M., Nesvag, R., Hagler, D. J., Jr., Bergmann, O., Fennema-Notestine, C., Hartberg, C. B., & Dale, A. M. (2012). Cortical volume, surface area, and thickness in schizophrenia and bipolar disorder. [Research Support, Non-U.S. Gov't]. *Biological Psychiatry*, 71(6), 552–560. doi:10.1016/j.biopsych.2011.11.026.
- Robinson, H., Calamia, M., Glascher, J., Bruss, J., & Tranel, D. (2014). Neuroanatomical correlates of executive functions: a neuropsychological approach using the EXAMINER battery. [Research Support, N.I.H., Extramural Research Support, Non-U.S. Gov't]. *Journal of International Neuropsychological Society*, 20(1), 52–63. doi:10.1017/S135561771300060X.
- Rogalski, E., Cobia, D., Martersteck, A., Rademaker, A., Wieneke, C., Weintraub, S., & Mesulam, M. M. (2014). Asymmetry of cortical decline in subtypes of primary progressive aphasia. [Research Support, N.I.H., Extramural]. *Neurology*, 83(13), 1184–1191. doi:10.1212/WNL.0000000000000824.
- Rogalsky, C., Poppa, T., Chen, K. H., Anderson, S. W., Damasio, H., Love, T., & Hickok, G. (2015). Speech repetition as a window on the neurobiology of auditory-motor integration for speech: a voxel-based lesion symptom mapping study. *Neuropsychologia*, 71, 18–27. doi:10.1016/j.neuropsychologia.2015.03.012.
- Rombaux, P., Huart, C., De Volder, A. G., Cuevas, I., Renier, L., Duprez, T., & Grandin, C. (2010). Increased olfactory bulb volume and olfactory function in early blind subjects. *Neuroreport*, 21(17), 1069–1073. doi:10.1097/WNR.0b013e32833fcba.
- Rosenbloom, M., Sullivan, E. V., & Pfefferbaum, A. (2003). Using magnetic resonance imaging and diffusion tensor imaging to assess brain damage in alcoholics. [Comparative Study Research Support, U.S. Gov't, P.H.S. Review]. *Alcohol Research and Health The Journal of the National Institute on Alcohol Abuse and Alcoholism*, 27(2), 146–152.
- Sastre-Garriga, J., Arevalo, M. J., Renom, M., Alonso, J., Gonzalez, I., Galan, I., & Rovira, A. (2009). Brain volumetry counterparts of cognitive impairment in patients with multiple sclerosis. [Research Support, Non-U.S. Gov't]. *Journal of Neurological Sciences*, 282(1-2), 120–124. doi:10.1016/j.jns.2008.12.019.
- Scarpazza, C., Tognin, S., Frisciata, S., Sartori, G., & Mechelli, A. (2015). False positive rates in voxel-based morphometry studies of the human brain: should we be worried? [Research Support, Non-U.S. Gov't Review]. *Neuroscience and Biobehavioral Reviews*, 52, 49–55. doi:10.1016/j.neubiorev.2015.02.008.
- Scheltens, P., Barkhof, F., Leys, D., Prupo, J. P., Nauta, J. J., Vermersch, P., & Valk, J. (1993). A semiquantitative rating scale for the assessment of signal hyperintensities on magnetic resonance imaging. *Journal of Neurological Sciences*, 114(1), 7–12.
- Scheltens, P., Launer, L. J., Barkhof, F., Weinstein, H. C., & van Gool, W. A. (1995). Visual assessment of medial temporal lobe atrophy on magnetic resonance imaging: interobserver reliability. *Journal of Neurology*, 242(9), 557–560.
- Schmidt, M. J., Langen, N., Klumpp, S., Nasirimanesh, F., Shirvanchi, P., Ondreka, N., & Kramer, M. (2012a). A study of the comparative anatomy of the brain of domestic ruminants using magnetic resonance imaging. *The Veterinary Journal*, 191(1), 85–93. doi:10.1016/j.tvjl.2010.12.026.
- Schmidt, P., Gaser, C., Arsic, M., Buck, D., Forschler, A., Berthele, A., & Muhlau, M. (2012b). An automated tool for detection of FLAIR-hyperintense white-matter lesions in multiple sclerosis. *NeuroImage*, 59(4), 3774–3783. doi:10.1016/j.neuroimage.2011.11.032.
- Shah, A., Jung, H., & Li, G. (2015). Impact of world war I on brain mapping. *Journal of Neurosurgical Sciences*.
- Shallice, T. (1988). *From neuropsychology to mental structure*. New York: Cambridge University Press.
- Shear, P. K., Jernigan, T. L., & Butters, N. (1994). Volumetric magnetic resonance imaging quantification of longitudinal brain changes in abstinent alcoholics. [Research Support, U.S. Gov't, Non-P.H.S. Research Support, U.S. Gov't, P.H.S.]. *Alcoholism: Clinical and Experimental Research*, 18(1), 172–176.
- Shenton, M. E., Kikinis, R., Jolesz, F. A., Pollak, S. D., LeMay, M., Wible, C. G., et al. (1992). Abnormalities of the left temporal lobe and thought disorder in schizophrenia. A quantitative magnetic resonance imaging study. [Research Support, Non-U.S. Gov't Research Support, U.S. Gov't, Non-P.H.S. Research Support, U.S. Gov't, P.H.S.]. *The New England Journal of Medicine*, 327(9), 604–612. doi:10.1056/NEJM19920827327095.
- Shi, L., Wang, D., Liu, S., Pu, Y., Wang, Y., Chu, W. C., & Ahuja, A. T. (2013). Automated quantification of white matter lesion in magnetic resonance imaging of patients with acute infarction. [Research Support, Non-U.S. Gov't]. *Journal of Neuroscience Methods*, 213(1), 138–146. doi:10.1016/j.jneumeth.2012.12.014.
- Shimamura, A. P., Jernigan, T. L., & Squire, L. R. (1988). Korsakoff's syndrome: radiological (CT) findings and neuropsychological correlates. [Research Support, U.S. Gov't, Non-P.H.S. Research Support, U.S. Gov't, P.H.S.]. *Journal of Neuroscience*, 8(11), 4400–4410.
- Squeglia, L. M., Jacobus, J., Sorg, S. F., Jernigan, T. L., & Tapert, S. F. (2013). Early adolescent cortical thinning is related to better neuropsychological performance. [Research Support, N.I.H., Extramural]. *Journal of International Neuropsychological Society*, 19(9), 962–970. doi:10.1017/S1355617713000878.

- Stephan, H., Frahm, H. D., & Baron, G. (1987). Comparison of brain structure volumes in Insectivora and primates. VII. Amygdaloid components. *Journal für Hirnforschung*, 28(5), 571–584.
- Stiles, J., & Jernigan, T. L. (2010). The basics of brain development. *Neuropsychology Review*, 20(4), 327–348. doi:10.1007/s11065-010-9148-4.
- Streitburger, D. P., Moller, H. E., Tittgemeyer, M., Hund-Georgiadis, M., Schroeter, M. L., & Mueller, K. (2012). Investigating structural brain changes of dehydration using voxel-based morphometry. *PLoS ONE*, 7(8), e44195. doi:10.1371/journal.pone.0044195.
- Sui, J., Pearlson, G. D., Du, Y., Yu, Q., Jones, T. R., Chen, J., & Calhoun, V. D. (2015). In search of multimodal neuroimaging biomarkers of cognitive deficits in schizophrenia. *Biological Psychiatry*. doi:10.1016/j.biopsych.2015.02.017.
- Sullivan, E. V., & Pfefferbaum, A. (2007). Neuroradiological characterization of normal adult ageing. [Research Support, N.I.H., Extramural Review]. *British Journal of Radiology*, 80 Spec No 2, S99–108. doi: 10.1259/bjr/22893432
- Suppa, P., Anker, U., Spies, L., Bopp, I., Ruegger-Frey, B., Klaghoffer, R., & Buchert, R. (2015). Fully automated atlas-based hippocampal volumetry for detection of Alzheimer's disease in a memory clinic setting. [Research Support, Non-U.S. Gov't]. *Journal of Alzheimer's Disease JAD*, 44(1), 183–193. doi:10.3233/JAD-141446.
- Synek, V., Reuben, J. R., & Du Boulay, G. H. (1976). Comparing Evans' index and computerized axial tomography in assessing relationship of ventricular size to brain size. *Neurology*, 26(3), 231–233.
- Taki, Y., Hashizume, H., Sassa, Y., Takeuchi, H., Asano, M., Asano, K., & Kawashima, R. (2012). Correlation among body height, intelligence, and brain gray matter volume in healthy children. *NeuroImage*, 59(2), 1023–1027. doi:10.1016/j.neuroimage.2011.08.092.
- Tate, D. F., Khedraki, R., Neeley, E. S., Ryser, D. K., & Bigler, E. D. (2011). Cerebral volume loss, cognitive deficit, and neuropsychological performance: comparative measures of brain atrophy: II. Traumatic brain injury. *Journal of International Neuropsychological Society*, 17(2), 308–316. doi:10.1017/S1355617710001670.
- Tate, D. F., York, G. E., Reid, M. W., Cooper, D. B., Jones, L., Robin, D. A., & Lewis, J. (2014). Preliminary findings of cortical thickness abnormalities in blast injured service members and their relationship to clinical findings. [Research Support, Non-U.S. Gov't]. *Brain Imaging and Behavior*, 8(1), 102–109. doi:10.1007/s11682-013-9257-9.
- Teuber, H. L. (2009). The riddle of frontal lobe function in man. 1964. [Biography Classical Article Historical Article Research Support, N.I.H., Extramural Research Support, Non-U.S. Gov't Research Support, U.S. Gov't, Non-P.H.S.]. *Neuropsychology Review*, 19(1), 25–46.
- Toga, A. W. (2015). *Brain mapping: An encyclopedic reference*. New York: Elsevier.
- Toga, A. W., & Thompson, P. M. (2005). Genetics of brain structure and intelligence. [Research Support, N.I.H., Extramural Research Support, U.S. Gov't, P.H.S. Review]. *Annual Review of Neuroscience*, 28, 1–23. doi:10.1146/annurev.neuro.28.061604.135655.
- Tooth, G. (1947). On the use of mental tests for the measurement of disability after head injury, with a comparison between the results of these tests in patients after head injury and psychoneurotics. *Journal of Neurology, Neurosurgery, and Psychiatry*, 10(1), 1–11.
- Turkheimer, E., Cullum, C. M., Hubler, D. W., Paver, S. W., Yeo, R. A., & Bigler, E. D. (1984). Quantifying cortical atrophy. *Journal of Neurology, Neurosurgery, and Psychiatry*, 47(12), 1314–1318.
- Tustison, N. J., Cook, P. A., Klein, A., Song, G., Das, S. R., Duda, J. T., & Avants, B. B. (2014). Large-scale evaluation of ANTs and FreeSurfer cortical thickness measurements. *NeuroImage*, 99, 166–179. doi:10.1016/j.neuroimage.2014.05.044.
- Varoquaux, G., & Thirion, B. (2014). How machine learning is shaping cognitive neuroimaging. [Review]. *GigaScience*, 3, 28. doi:10.1186/2047-217X-3-28.
- Voevodskaya, O., Simmons, A., Nordenskjold, R., Kullberg, J., Ahlstrom, H., Lind, L., & Westman, E. (2014). The effects of intracranial volume adjustment approaches on multiple regional MRI volumes in healthy aging and Alzheimer's disease. *Frontiers in Aging Neuroscience*, 6, 264. doi:10.3389/fnagi.2014.00264.
- von der Hagen, M., Pivarcsi, M., Liebe, J., von Bernuth, H., Didonato, N., Hennermann, J. B., & Kaindl, A. M. (2014). Diagnostic approach to microcephaly in childhood: a two-center study and review of the literature. *Developmental Medicine and Child Neurology*, 56(8), 732–741. doi:10.1111/dmcn.12425.
- Walser, R. L., & Ackerman, L. V. (1977). Determination of volume from computerized tomograms: finding the volume of fluid-filled brain cavities. *Journal of Computer Assisted Tomography*, 1(1), 117–130.
- Wechsler, D. (1999). *Wechsler abbreviated scale of intelligence (WASI)*. San Antonio: Pearson.
- Wenger, E., Martensson, J., Noack, H., Bodammer, N. C., Kuhn, S., Schaefer, S., & Lovden, M. (2014). Comparing manual and automatic segmentation of hippocampal volumes: reliability and validity issues in younger and older brains. [Comparative Study Research Support, Non-U.S. Gov't Validation Studies]. *Human Brain Mapping*, 35(8), 4236–4248. doi:10.1002/hbm.22473.
- Wilde, E. A., Hunter, J. V., & Bigler, E. D. (2012). A primer of neuroimaging analysis in neurorehabilitation outcome research. *NeuroRehabilitation*, 31(3), 227–242. doi:10.3233/NRE-2012-0793.
- Wilde, E. A., Hunter, J. V., & Bigler, E. D. (2014). Neuroimaging in traumatic brain injury. In M. Sherer & A. M. Sander (Eds.), *Handbook on the neuropsychology of traumatic brain injury* (pp. 111–136). New York: Springer.
- Wilke, M., de Haan, B., Juenger, H., & Karnath, H. O. (2011). Manual, semi-automated, and automated delineation of chronic brain lesions: a comparison of methods. [Comparative Study Research Support, Non-U.S. Gov't]. *NeuroImage*, 56(4), 2038–2046. doi:10.1016/j.neuroimage.2011.04.014.
- Willerman, L., Schultz, R., Rutledge, J. N., & Bigler, E. D. (1991). In vivo brain size and intelligence. *Intelligence*, 15(223–228).
- Wisse, L. E., Biessels, G. J., & Geerlings, M. I. (2014). A critical appraisal of the hippocampal subfield segmentation package in FreeSurfer. [Review]. *Frontiers in Aging Neuroscience*, 6, 261. doi:10.3389/fnagi.2014.00261.
- Wu, Y., Du, H., Storey, P., Glielmi, C., Malone, F., Sidharthan, S., & Edelman, R. R. (2012). Comprehensive brain analysis with automated high-resolution magnetization transfer measurements. *Journal of Magnetic Resonance Imaging*, 35(2), 309–317. doi:10.1002/jmri.22835.
- Zahodne, L. B., Manly, J. J., Narkhede, A., Griffith, E. Y., DeCarli, C., Schupf, N. S., ... Brickman, A. M. (2015). Structural MRI predictors of late-life cognition differ across African Americans, Hispanics, and Whites. *Current Alzheimer Research*.
- Zangwill, O. L. (1945). Psychological work at the edinburgh brain injuries unit. *British Medical Journal*, 2(4416), 248–251.
- Zatz, L. M., Jernigan, T. L., & Ahumada, A. J., Jr. (1982a). Changes on computed cranial tomography with aging: intracranial fluid volume. [Research Support, U.S. Gov't, Non-P.H.S.]. *AJNR - American Journal of Neuroradiology*, 3(1), 1–11.
- Zatz, L. M., Jernigan, T. L., & Ahumada, A. J., Jr. (1982b). White matter changes in cerebral computed tomography related to aging. [Research Support, U.S. Gov't, Non-P.H.S.]. *Journal of Computer Assisted Tomography*, 6(1), 19–23.
- Zipursky, R. B., Marsh, L., Lim, K. O., DeMent, S., Shear, P. K., Sullivan, E. V., & Pfefferbaum, A. (1994). Volumetric MRI assessment of temporal lobe structures in schizophrenia. *Biological Psychiatry*, 35(8), 501–516.